A full analytical solution for the force-driven compressible Poiseuille gas flow based on a nonlinear coupled constitutive relation

R. S. Myong[a)]
Department of Mechanical and Aerospace Engineering, Research Center for Aircraft Parts Technology, Gyeongsang National University, Jinju, Gyeongnam 660-701, South Korea

(Received 22 June 2010; accepted 3 December 2010; published online 24 January 2011)

The compressible Poiseuille gas flow driven by a uniform force is analytically investigated using a phenomenological nonlinear coupled constitutive relation model. A new fully analytical solution in compact tangent (or hyperbolic tangent in the case of diatomic gases) functional form explains the origin behind the central temperature minimum and a heat transfer from the cold region to the hot region. The solution is not only proven to satisfy the conservation laws exactly but also well-defined for all physical conditions (the Knudsen number and a force-related dimensionless parameter). It is also shown that the non-Fourier law associated with the coupling of force and viscous shear stress in the constitutive relation is responsible for the existence of the central temperature minimum, while a kinematic constraint on viscous shear and normal stresses identified in the velocity shear flow is the main source of the nonuniform pressure distribution. In addition, the convex pressure profile with a maximum at the center is theoretically predicted for diatomic gases. Finally, the existence of the Knudsen minimum in the mass flow rate is demonstrated by developing an exact analytical formula for the average temperature of the bulk flow. © *2011 American Institute of Physics*. [doi:10.1063/1.3540671]

I. INTRODUCTION

Recently, new developments have been reported on the constitutive relations[1] of gases in a thermal nonequilibrium (rarefied and microscale) from the viewpoint of the modified moment method to the Boltzmann equation.[2–7] An important result obtained from these works[5–7] is that constitutive relations between stresses (heat flux) and the strain rate (the temperature gradient) are generally nonlinear and coupled in states removed from thermal equilibrium. Furthermore, the nonlinear coupled (algebraic) constitutive relations[7] (called NCCRs hereafter) showed that the subtle interplay of various terms appearing in the constitutive equations is the dominant factor in determining the effectiveness of the constitutive models. When the constitutive relations were applied to the compression-dominated shock structure problem as a test case, it was found that they successfully yield shock structures over the entire range of Mach numbers and for all gases.[3–6] However, as recent interests shift to the fundamental physics of gas transport in micro- and nanodevices,[8,9] the question of the applicability of the new constitutive relations to the velocity shear-dominated flow problems[10–16] has emerged. With the aim of answering the aforementioned question, a benchmark problem known in literature as the force-driven Poiseuille gas flow[12,14,17–22] is investigated in the present study.

The force-driven *compressible* Poiseuille flow, as illustrated in Fig. 1, is defined as a stationary flow in a slab under the action of a *constant* external force parallel to the walls. It is a simple, albeit very instructive, problem in the sense that it is purely one dimensional but brings out the essence of the nonclassical constitutive relations in states removed from thermal equilibrium. For example, the classical hydrodynamic theory is unable to predict the nonuniform pressure distribution and the nonmonotonic temperature distribution near the centerline. Efforts to solve this dilemma have led to the development of various methods including the Super-Burnett equations,[12] the Brenner's hydrodynamic model,[14] the regularized moment equations,[17] the perturbation theory,[18,19] the direct simulation Monte Carlo (DSMC),[20,21] and the lattice Boltzmann method.[22] However, since most previous studies have been conducted by approximate methods, such as numerical simulations, the exact underlying physics of these abnormal properties and the nature of analytical solution are not fully understood, as noted by Ansumali.[22] The goal of obtaining better understanding and proving the existence of analytical solution for all physical conditions (the Knudsen number and a force-related dimensionless parameter) is pursued here by developing a fully analytical solution for the conservation laws in conjunction with the nonlinear coupled constitutive relation.

II. PHENOMENOLOGICAL NCCR MODEL FOR THE VELOCITY SHEAR GAS FLOW

When the external force $\mathbf{a}$ is present, it affects not only the conservation laws but also the kinetic equation (or the corresponding constitutive relations). Therefore, the Boltzmann kinetic equation of the distribution of monatomic gas particles $f(\mathbf{v};\mathbf{r},t)$ must read as follows, in particular, with an extra term $\mathbf{a}\cdot\nabla_{\mathbf{v}}f$:

[a)]Electronic mail: myong@gnu.ac.kr.

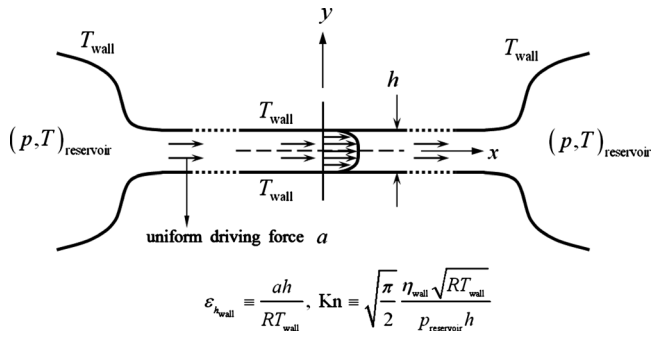

FIG. 1. Sketch of the one-dimensional fully developed compressible Poiseuille gas flow in rectangular channel (driven by uniform force) between two pressure-regulated reservoirs.

$$\left[\frac{\partial}{\partial t} + \mathbf{v}\cdot\nabla + \mathbf{a}\cdot\nabla_{\mathbf{v}}\right] f(\mathbf{v},\mathbf{r},t) = C[f], \tag{2.1}$$

where the term $C[f]$ represents the collision integral of the interaction among the particles. By utilizing the collision invariants of the Boltzmann equation, the following conservation laws can be derived:

$$\rho\frac{D}{Dt}\begin{bmatrix}1/\rho\\ \mathbf{u}\\ E_t\end{bmatrix} + \nabla\cdot\begin{bmatrix}\mathbf{u}\\ \mathbf{P}\\ \mathbf{P}\cdot\mathbf{u}+\mathbf{Q}\end{bmatrix} = \begin{bmatrix}0\\ \rho\mathbf{a}\\ \rho\mathbf{a}\cdot\mathbf{u}\end{bmatrix}. \tag{2.2}$$

In this expression, ρ and $\mathbf{u}$ denote the density and the average velocity vector, respectively. E_t and D/Dt denote the total energy and the material time derivative, respectively. $\mathbf{P}$ and $\mathbf{Q}$ are the stress tensor and the heat flux vector statistically defined by the formulas

$$\mathbf{P} \equiv \langle m\mathbf{cc}f\rangle, \quad \mathbf{Q} \equiv \left\langle \tfrac{1}{2}mc^2\mathbf{c}f\right\rangle,$$

respectively, where m and $\mathbf{c}$ denote the molecular mass and the peculiar velocity of the molecule, respectively. An abbreviation is used for the integration over $\mathbf{v}$ space with angular brackets $\langle\cdots\rangle = \int d\mathbf{v}\cdots$. In the case of dilute monatomic gases, the stress tensor can be further decomposed into two components; pressure and traceless parts,

$$\mathbf{P} \equiv p\mathbf{I} + \mathbf{\Pi},$$

where the statistical mechanical formulas for p and $\mathbf{\Pi}$ are, respectively,

$$p \equiv \left\langle \tfrac{1}{3}m\ \mathrm{Tr}(\mathbf{cc})f\right\rangle, \quad \mathbf{\Pi} \equiv \langle m[\mathbf{cc}]^{(2)}f\rangle.$$

Here, the symbol $[\ ]^{(2)}$ stands for a traceless symmetric part of the tensor. In the case of a dilute gas, the pressure p and the temperature T are related by the ideal-gas equation of state. The derivation of constitutive relations can be done by applying the so-called Maxwell–Grad moment method, which was first introduced by Maxwell (the so-called equation of change) and later refined by Grad.[23] However, a slightly different method called the modified moment method developed recently by Eu[2,3] will be adopted in the present study. A detailed description is repeated here for the purpose of highlighting the effect of the external force $\mathbf{a}$ and showing exactly where the closure or approximations are introduced in the derivation. The modified moment method (Ref. 2, pp. 348–386) starts with differentiating the statistical definition of variable in question and later combining with the Boltzmann equation, in contrast to taking first the velocity moments of the Boltzmann equation in the conventional Maxwell–Grad method. For the stress tensor $\mathbf{P}$, it yields

$$\begin{aligned}\frac{\partial\mathbf{P}}{\partial t} &= -\langle m\mathbf{cc}(\mathbf{v}\cdot\nabla + \mathbf{a}\cdot\nabla_{\mathbf{v}})f\rangle + \left\langle f\frac{\partial(m\mathbf{cc})}{\partial t}\right\rangle + \mathbf{\Lambda}^{(P)}\\ &= -\nabla\cdot\langle\mathbf{u}m\mathbf{cc}f\rangle - \nabla\cdot\langle\mathbf{c}m\mathbf{cc}f\rangle\\ &\quad + \left\langle f\left(\frac{D}{Dt} + \mathbf{c}\cdot\nabla + \mathbf{a}\cdot\nabla_{\mathbf{v}}\right)m\mathbf{cc}\right\rangle + \mathbf{\Lambda}^{(P)},\end{aligned} \tag{2.3}$$

where $\mathbf{\Lambda}^{(P)} \equiv \langle m\mathbf{cc}C[f]\rangle$. The second and third terms on the right-hand side are called the kinematic term since it stems from the streaming effect of the particle motion. When the third term on the right-hand side is expanded further, Eq. (2.3) is reduced to

$$\frac{\partial\mathbf{P}}{\partial t} = -\nabla\cdot(\mathbf{uP}) - \nabla\cdot\boldsymbol{\psi}^{(P)} - [\mathbf{P}\cdot\nabla\mathbf{u} + (\nabla\mathbf{u})^T\cdot\mathbf{P}] + \mathbf{\Lambda}^{(P)}, \tag{2.4}$$

where $\boldsymbol{\psi}^{(P)} \equiv \langle m\mathbf{ccc}f\rangle$. When the nonequilibrium part of the stress $\mathbf{\Pi}$ instead of the stress tensor $\mathbf{P}$ is considered, the corresponding constitutive equation can be obtained by subtracting the trace part of the tensor $\mathbf{P}$,

$$\begin{aligned}\frac{\partial\mathbf{\Pi}}{\partial t} &= -\nabla\cdot(\mathbf{u\Pi}) - \nabla\cdot\boldsymbol{\psi}^{(\Pi)} - 2[\mathbf{\Pi}\cdot\nabla\mathbf{u}]^{(2)} - 2p[\nabla\mathbf{u}]^{(2)}\\ &\quad + \mathbf{\Lambda}^{(\Pi)},\end{aligned} \tag{2.5}$$

where

$$\boldsymbol{\psi}^{(\Pi)} \equiv \langle m[\mathbf{cc}]^{(2)}\mathbf{c}f\rangle = \boldsymbol{\psi}^{(P)} - \tfrac{1}{3}\mathbf{I}\langle m\ \mathrm{Tr}(\mathbf{ccc})f\rangle$$

and $\mathbf{\Lambda}^{(\Pi)} \equiv \langle m[\mathbf{cc}]^{(2)}C[f]\rangle$. Note that Eq. (2.5) is exactly the same as Eq. (5.15) in Grad's work.[23] Similarly, by starting from the statistical definition of heat flux vector $\mathbf{Q}$, the constitutive equation of heat flux can be expressed as

$$\begin{aligned}\frac{\partial\mathbf{Q}}{\partial t} &= -\nabla\cdot(\mathbf{uQ}) - \nabla\cdot\boldsymbol{\psi}^{(Q)} - \boldsymbol{\psi}^{(P)}:\nabla\mathbf{u} - C_p\mathbf{\Pi}\cdot\nabla T\\ &\quad - \mathbf{Q}\cdot\nabla\mathbf{u} - \left(\frac{D\mathbf{u}}{Dt} - \mathbf{a}\right)\cdot\mathbf{\Pi} - C_p p\nabla T + \mathbf{\Lambda}^{(Q)},\end{aligned} \tag{2.6}$$

where $\boldsymbol{\psi}^{(Q)} \equiv \left\langle \tfrac{1}{2}mc^2\mathbf{c}\mathbf{c}f\right\rangle$ and $\mathbf{\Lambda}^{(Q)} \equiv \left\langle \tfrac{1}{2}mc^2\mathbf{c}C[f]\right\rangle$. C_p is the heat capacity per mass at constant pressure. Equations (2.2), (2.5), and (2.6) can be expressed in another instructive form

$$\rho\frac{D}{Dt}\begin{bmatrix}1/\rho\\ \mathbf{u}\\ E_t\end{bmatrix}+\nabla\cdot\begin{bmatrix}\mathbf{u}\\ p\mathbf{I}\\ p\mathbf{u}\end{bmatrix}=-\nabla\cdot\begin{bmatrix}0\\ \boldsymbol{\Pi}\\ \mathbf{Q}+\boldsymbol{\Pi}\cdot\mathbf{u}\end{bmatrix}+\begin{bmatrix}0\\ \rho\mathbf{a}\\ \rho\mathbf{a}\cdot\mathbf{u}\end{bmatrix},$$

$$\rho\frac{D}{Dt}\begin{bmatrix}\boldsymbol{\Pi}/\rho\\ \mathbf{Q}/\rho\end{bmatrix}=-\nabla\cdot\begin{bmatrix}\boldsymbol{\psi}^{(\Pi)}\\ \boldsymbol{\psi}^{(Q)}\end{bmatrix}-\begin{bmatrix}0\\ \boldsymbol{\psi}^{(P)}:\nabla\mathbf{u}\end{bmatrix}-\begin{bmatrix}2[\boldsymbol{\Pi}\cdot\nabla\mathbf{u}]^{(2)}\\ C_p\boldsymbol{\Pi}\cdot\nabla T+\mathbf{Q}\cdot\nabla\mathbf{u}+\dfrac{D\mathbf{u}}{Dt}\cdot\boldsymbol{\Pi}\end{bmatrix}+\begin{bmatrix}0\\ \mathbf{a}\cdot\boldsymbol{\Pi}\end{bmatrix}-\begin{bmatrix}2p[\nabla\mathbf{u}]^{(2)}\\ pC_p\nabla T\end{bmatrix}+\begin{bmatrix}\boldsymbol{\Lambda}^{(\Pi)}\\ \boldsymbol{\Lambda}^{(Q)}\end{bmatrix}.$$

It is interesting to note that no terms associated with the external force **a** appear in the constitutive relation of shear stress $\boldsymbol{\Pi}$ since $\langle mf(\mathbf{a}\cdot\nabla_{\mathbf{v}})[\mathbf{cc}]^{(2)}\rangle=0$, while a new term $\mathbf{a}\cdot\boldsymbol{\Pi}$ appears in the constitutive relation of heat flux **Q**.

Up to now, no approximations are made in the process, and therefore the constitutive equations (2.5) and (2.6) are a direct consequence of the Boltzmann equation. They are, however, an open system of partial differential equations; thus, a proper closure must be introduced so that it may be used as a practical constitutive equation. There exist various methods[2–4,15,23–26] to achieve this goal, for example, mathematically motivated Grad's closure,[23] but it is generally accepted that there exists no single closure theory founded on a firm theoretical justification. For this reason, we will follow the tradition that, in natural science, the difference between theoretical truth and pure mathematical speculation is eventually decided by empirical evidence. In other words, the justification of the theoretical model is *a posteriori* and will be determined afterward by its ability to describe properties experimentally studied. In the present work, physical observations for *relative importance* of various terms appearing in the constitutive equations will be imposed on the closure.

By the steady-state and pure one-dimensional assumption of the Poiseuille flow, that is, all variables depending on the coordinate y only, the substantial derivative of shear stress and heat flux will vanish since the convective derivatives $\mathbf{u}\cdot\nabla$ are zero by definition ($v=w=0,\ \partial/\partial x=\partial/\partial z=0$). Also, the terms associated with $\boldsymbol{\psi}^{(\Pi),(P)}$ and $\boldsymbol{\psi}^{(Q)}$ in Eqs. (2.5) and (2.6), which are one order higher than the dependent variables $\boldsymbol{\Pi}$ and **Q**, respectively, may be assumed small; that is,

$$\nabla\cdot\boldsymbol{\psi}^{(\Pi)}\approx 0,\qquad \nabla\cdot\boldsymbol{\psi}^{(Q)}+\boldsymbol{\psi}^{(P)}:\nabla\mathbf{u}\approx 0. \tag{2.7}$$

Here, it must be emphasized that this approximation does not imply zero shear stress $\boldsymbol{\Pi}$ or heat flux vector **Q**, which are fundamental variables to be determined by the constitutive equations themselves. Also, it must be noted that $\boldsymbol{\psi}^{(\Pi),(P)}$ and $\boldsymbol{\psi}^{(Q)}$ are allowed to remain finite under the closure (2.7). In fact, the closure (2.7) is not unprecedented since a similar practice was used in the past when the (inviscid) Euler equation is derived from the (viscous) Navier–Stokes–Fourier equation. In such a case, the $\nabla\cdot\boldsymbol{\Pi}$ appearing in the conservation law of momentum, which is the divergence of shear stress tensor $\boldsymbol{\Pi}$, one order higher than the dependent variable **u**, was assumed small. Also, the validity of this approximation can be confirmed when the terms are written in component form for pure one-dimensional flow ($dc_x/dy=-du/dy,\ dc_{y,z}/dy=0$),

$$\nabla\cdot\boldsymbol{\psi}^{(\Pi)}=\frac{d}{dy}\begin{bmatrix}\langle mc_x^2c_yf\rangle-\frac{1}{3}\langle mc^2c_yf\rangle & \langle mc_y^2c_xf\rangle & \langle mc_xc_yc_zf\rangle\\ \langle mc_y^2c_xf\rangle & \langle mc_y^3f\rangle-\frac{1}{3}\langle mc^2c_yf\rangle & \langle mc_y^2c_zf\rangle\\ \langle mc_xc_yc_zf\rangle & \langle mc_y^2c_zf\rangle & \langle mc_z^2c_yf\rangle-\frac{1}{3}\langle mc^2c_yf\rangle\end{bmatrix},$$

$$\nabla\cdot\boldsymbol{\psi}^{(Q)}+\boldsymbol{\psi}^{(P)}:\nabla\mathbf{u}=\frac{d}{dy}\begin{bmatrix}\langle mc^2c_xc_yf/2\rangle\\ \langle mc^2c_y^2f/2\rangle\\ \langle mc^2c_yc_zf/2\rangle\end{bmatrix}+\frac{du}{dy}\begin{bmatrix}\langle mc_x^2c_yf\rangle\\ \langle mc_xc_y^2f\rangle\\ \langle mc_xc_yc_zf\rangle\end{bmatrix}.$$

It can be noticed that all components, for example, $[\nabla\cdot\boldsymbol{\psi}^{(\Pi)}]_{xy}=d\langle mc_y^2c_xf\rangle/dy$, the spatial derivative of the macroscopic quantity $\langle mc_y^2c_xf\rangle$, remain small in comparison with $2[\boldsymbol{\Pi}\cdot\nabla\mathbf{u}]_{xy}^{(2)}=-\langle mc_y^2f\rangle du/dy$ and become strictly zero in local thermal equilibrium ($du/dy=0,\ df/dy=0$). It can be noted that the closure (2.7) is the same, in principle, as that proposed first by Eu[3,25] in his generalized hydrodynamic theory of shock waves. With this approximation, the one-dimensional constitutive equations for the steady-state constant force-driven compressible Poiseuille gas flow are reduced to

$$\begin{bmatrix}0\\ 0\end{bmatrix}=-\begin{bmatrix}2[\boldsymbol{\Pi}\cdot\nabla\mathbf{u}]^{(2)}\\ C_p\boldsymbol{\Pi}\cdot\nabla T+\mathbf{Q}\cdot\nabla\mathbf{u}\end{bmatrix}-\begin{bmatrix}0\\ a\mathbf{I}\cdot\boldsymbol{\Pi}\end{bmatrix}-p\begin{bmatrix}2[\nabla\mathbf{u}]^{(2)}\\ C_p\nabla T\end{bmatrix}+\begin{bmatrix}\boldsymbol{\Lambda}^{(\Pi)}\\ \boldsymbol{\Lambda}^{(Q)}\end{bmatrix}. \tag{2.8}$$

It will be shown later that this constitutive model based on the aforementioned approximations is suitable for fully analytical approach due to its algebraic nature and is just enough to describe most of qualitative properties of the force-driven compressible Poiseuille gas flow predicted by DSMC. How-

ever, if numerical approach is preferred over fully analytical approach, one can either relax some of the approximations employed in this study or search for more accurate closure with the possibility of additional complexity arising from the partial differential nature of the constitutive equation. Finally, constitutive equations can be written in the following *algebraic* relations:

$$\begin{bmatrix} 0 \\ 0 \end{bmatrix} = -\begin{bmatrix} \underline{2p[\nabla \mathbf{u}]^{(2)}} + 2[\boldsymbol{\Pi} \cdot \nabla \mathbf{u}]^{(2)} \\ \underline{pC_p \nabla T} + \boldsymbol{\Pi} \cdot C_p \nabla T + \mathbf{Q} \cdot \nabla \mathbf{u} - a\mathbf{I} \cdot \boldsymbol{\Pi} \end{bmatrix} + \begin{bmatrix} \boldsymbol{\Lambda}^{(\Pi)} \\ \boldsymbol{\Lambda}^{(Q)} \end{bmatrix} \tag{2.9}$$

or in component form (Pr, Prandtl number)

$$\begin{bmatrix} 0 \\ 0 \\ 0 \\ 0 \\ 0 \\ 0 \\ 0 \\ 0 \\ 0 \end{bmatrix} = \begin{bmatrix} \underline{0} + 4\Pi_{xy}\Pi_{xy_0}/(3\eta) \\ \underline{0} - 2\Pi_{xy}\Pi_{xy_0}/(3\eta) \\ \underline{0} - 2\Pi_{xy}\Pi_{xy_0}/(3\eta) \\ \underline{p\Pi_{xy_0}/\eta} + \Pi_{yy}\Pi_{xy_0}/\eta \\ \underline{0} + \Pi_{yz}\Pi_{xy_0}/\eta \\ \underline{0} \\ \underline{0} + \Pi_{xy}C_pQ_{y_0}/k + C_pQ_y\Pi_{xy_0}/(\mathrm{Pr}\ \ k) + a\Pi_{xx} \\ \underline{pC_pQ_{y_0}/k} + \Pi_{yy}C_pQ_{y_0}/k + a\Pi_{xy} \\ \underline{0} + \Pi_{yz}C_pQ_{y_0}/k + a\Pi_{xz} \end{bmatrix} + \begin{bmatrix} \Lambda^{(\Pi_{xx})} \\ \Lambda^{(\Pi_{yy})} \\ \Lambda^{(\Pi_{zz})} \\ \Lambda^{(\Pi_{xy})} \\ \Lambda^{(\Pi_{xz})} \\ \Lambda^{(\Pi_{yz})} \\ \Lambda^{(Q_x)} \\ \Lambda^{(Q_y)} \\ \Lambda^{(Q_z)} \end{bmatrix}. \tag{2.10}$$

Here, the underlined terms represent the linear thermodynamic forces in the present velocity shear flow and they correspond to the Navier–Stokes–Fourier constitutive relations,

$$\boldsymbol{\Pi}_0 = -2\eta[\nabla \mathbf{u}]^{(2)} \quad \text{and} \quad \mathbf{Q}_0 = -k\nabla T. \tag{2.11}$$

With additional approximations $\boldsymbol{\Lambda}^{(\Pi)} = -p\boldsymbol{\Pi}/\eta$ and $\boldsymbol{\Lambda}^{(Q)} = -pC_p\mathbf{Q}/k$, where η and k represent the viscosity and the thermal conductivity, respectively, near local thermal equilibrium, the constitutive relations are proved to be inclusive of the Navier–Stokes–Fourier theory. Note that stress and heat flux are coupled to each other and are related nonlinearly to thermodynamic deriving forces in this algebraic system. Also, it can be observed that the constitutive relations are Galilean invariant since there exists no velocity term. This phenomenological NCCR model will be utilized to obtain full analytical solution for the force-driven compressible Poiseuille gas flow in a compact form.

III. CLASSICAL THEORY BASED ON NAVIER–STOKES–FOURIER RELATIONS

A. Conventional analytical solution for incompressible Navier–Stokes–Fourier relations

When the classical constitutive relations by Navier, Stokes, and Fourier are combined with the steady-state conservation law (2.2), the governing equation of the force-driven gaseous (monatomic) Poiseuille flow is reduced to the following system of ordinary differential equations:

$$\frac{d}{dy}\begin{bmatrix} \Pi_{xy} \\ p + \Pi_{yy} \\ \Pi_{yz} \\ \Pi_{xy}u + Q_y \end{bmatrix} = \begin{bmatrix} \rho a \\ 0 \\ 0 \\ \rho a u \end{bmatrix}, \quad \begin{bmatrix} 0 \\ 0 \\ 0 \\ 0 \\ 0 \end{bmatrix} = \begin{bmatrix} 0 \\ -\eta du/dy \\ 0 \\ 0 \\ -kdT/dy \end{bmatrix} - \begin{bmatrix} \Pi_{yy} \\ \Pi_{xy} \\ \Pi_{yz} \\ Q_x \\ Q_y \end{bmatrix}. \tag{3.1}$$

The combination of the second and fifth equations yields the uniform pressure distribution $p=p_m[\equiv p(y=0)]$ and $\Pi_{yy}=0$. It is also obvious that $\Pi_{yz}=Q_x=0$. The system is then simplified into the differential equations with the unknowns of the streamwise velocity u and the temperature T only. Then, the velocity solution in the function of the distance y from the wall of a slab $(-h/2\le y\le h/2)$ can be determined by solving the x-momentum equation with the Navier–Stokes law,

$$\frac{d}{dy}\left(-\eta\frac{du}{dy}\right)=\rho a \quad \text{or} \quad \Pi_{xy}=\rho a y. \tag{3.2}$$

Here, the density ρ is assumed constant. With the assumption of constant viscosity, the velocity profile is then determined as follows:

$$u(y)=u(0)-\frac{\rho a h^2}{\eta}\frac{(y/h)^2}{2}. \tag{3.3}$$

At this stage, it is necessary to specify the boundary condition for the velocity at the wall. It is well known that the slip boundary condition does not affect the qualitative aspect of pressure and temperature distributions in the central region,[22] which is the main interest in the study of the force-driven Poiseuille gas flow. However, a slip condition will be considered for the sake of completeness and quantitative comparison. Among various slip models, the Langmuir slip model based on the adsorption isotherm[27–31] is chosen in the present study since it is mathematically simple and, nonetheless, it turned out to be qualitatively the same as the conventional Maxwell slip model. With the slip model, the dimensionless slip velocity at the stationary wall surface can be expressed as

$$u(y=h/2)=(1-\alpha_V)u(y=0), \tag{3.4}$$

where

$$\alpha_V=\frac{\bar{\beta}_V}{1+\bar{\beta}_V}, \quad \bar{\beta}_V=\frac{1}{4\omega_V\ \mathrm{Kn}}, \quad \mathrm{Kn}=\sqrt{\frac{\pi}{2}}\frac{\eta_w\sqrt{RT_w}}{p_m h},$$

$$\text{and} \quad \omega_V=\omega_{V_0}(\nu)\exp\left(-\frac{D_e}{k_B T_w}\right).$$

The fraction of molecules at thermal equilibrium α_V is then reduced to

$$\alpha_V=\frac{1}{1+4\omega_V\ \mathrm{Kn}}.$$

Note that $\alpha_V\to 1$ and $\alpha_V\to 0$ in the limit of continuum and free-molecular flows, respectively. The coefficient ω_V,[28,29] which is a function of the inverse power law of the gas particle interaction potential ν and the adsorption potential parameter D_e, plays a role very similar to that of the slip coefficient σ_V defined as $(2-\phi_V)/\phi_V$, where ϕ_V is the momentum accommodation coefficient in the conventional Maxwell model. In fact, it is shown in Appendix A that with an equivalence condition $\sigma_V=\omega_V$,[28,29] the resulting velocity profile of the Maxwell slip model[32,33] is exactly the same as the following one of the Langmuir slip model:

$$u(y)=u(0)[1-4\alpha_V(y/h)^2] \quad \text{and} \quad \frac{\rho a h^2}{8\eta}=\alpha_V u(0). \tag{3.5}$$

The temperature profile can be obtained by first considering the energy equation in the conservation laws and then by combining it with the Navier–Stokes law. The resulting equation reduces to

$$\frac{dQ_y}{dy}=\frac{\Pi_{xy}^2}{\eta}, \tag{3.6}$$

and, when it is combined with Eq. (3.2) and is integrated once with respect to y, the heat flux in the y-direction can be written as

$$Q_y=\frac{\rho^2 a^2 h^3}{3\eta}(y/h)^3. \tag{3.7}$$

With the Fourier law and the assumption of *constant* thermal conductivity, the following temperature profile can be determined:

$$T(y)=T(0)-\frac{\rho^2 a^2 h^4}{12\eta k}(y/h)^4. \tag{3.8}$$

With the dimensionless temperature jump at the wall surface defined as

$$T(y=h/2)=\alpha_T T_w+(1-\alpha_T)T(y=0)$$

$$\text{and} \quad \alpha_T=\frac{1}{1+4\omega_T\ \mathrm{Kn}}, \tag{3.9}$$

the temperature profile can be expressed as

$$T(y)=T(0)-16\alpha_T[T(0)-T_w](y/h)^4$$

$$\text{and} \quad \frac{\rho^2 a^2 h^4}{192\eta k}=\alpha_T[T(0)-T_w]. \tag{3.10}$$

For this quartic profile, the average temperature can be easily calculated

$$T_{\mathrm{av}}\equiv\frac{\int_0^{h/2}T dy}{h/2}=T_w+\frac{\rho^2 a^2 h^4}{192\eta k}\frac{5-\alpha_T}{5\alpha_T}$$

$$\text{or} \quad \frac{T_w}{T_{\mathrm{av}}}=\left(1+\frac{\rho^2 a^2 h^4}{192\eta k T_w}\frac{5-\alpha_T}{5\alpha_T}\right)^{-1}. \tag{3.11}$$

It must be noted that the value T_{av} is well-defined for all physical conditions of ρ, a, h and is always greater than the wall temperature T_w. When it is combined with the relation (3.10), the following centerline temperature, which itself is the part of solution, can be determined:

$$T(0)=\frac{5T_{\mathrm{av}}-\alpha_T T_w}{5-\alpha_T}. \tag{3.12}$$

Notice also that the value $T(0)$ is well-defined for all physical conditions. Similar to the case of temperature, the centerline velocity can be determined by calculating the average velocity,

$$u_{\mathrm{av}} \equiv \frac{\int_0^{h/2} u dy}{h/2} = \frac{\rho a h^2}{8\eta}\frac{3-\alpha_V}{3\alpha_V} \quad \text{and} \quad u(0) = u_{\mathrm{av}}\frac{3}{3-\alpha_V}. \tag{3.13}$$

With these centerline values, the slip velocity and the temperature jump can be determined from Eqs. (3.4) and (3.9), respectively. Furthermore, the mass flow rate can be expressed as

$$\frac{\dot{m}/2h}{\rho_{\mathrm{av}}\sqrt{\gamma RT_w}} \equiv \frac{\int_0^{h/2} u dy}{2\sqrt{\gamma RT_w}h/2} = \frac{\rho a h^2}{16\eta\sqrt{\gamma RT_w}}\frac{(1-\alpha_V/3)}{\alpha_V}, \tag{3.14}$$

where γ is the specific heat ratio.

B. New analytical solution for compressible Navier–Stokes–Fourier relations

When compressible Navier–Stokes–Fourier relations are considered, it is critical to treat the temperature dependence of viscosity and thermal conductivity in a rigorous way. In the present study, a new method, which turned out to yield the exact solution both for the Navier-Stokes–Fourier equations and the new NCCR equations, is developed. Let us first introduce the following dimensionless variables and parameters:

$$y^* = y/h, \quad u^* = u/u_r, \quad T^* = T/T_r, \quad p^* = p/p_m,$$

$$\Pi^* = \Pi/(\eta_w u_r/h), \quad Q^* = Q/(k_w \Delta T/h), \tag{3.15}$$

$$\varepsilon_h = \frac{ah}{RT_r}, \quad M = \frac{u_r}{\sqrt{\gamma RT_w}}, \quad \mathrm{Kn} = \sqrt{\frac{\pi}{2}}\frac{\eta_w\sqrt{RT_w}}{p_m h},$$

$$N_\delta = \frac{\eta_w u_r/h}{p_m}, \quad \mathrm{Ec} = \frac{(\gamma-1)M^2}{\Delta T/T_w}, \quad \mathrm{Pr} = \frac{C_p\eta_w}{k_w},$$

where the subscripts r, w, and m denote the reference state, the state at the wall, and the state at the middle of a slab, that is, $y=0$, respectively. Here, ΔT denotes $|T_m - T_w|$. ε_h, M, N_δ, Kn, and Ec are dimensionless hydrodynamic numbers: a force-related number (similar to the Richardson number), Mach number, a composite number, Knudsen, and Eckert numbers, respectively. The composite number N_δ is related to other numbers such that $N_\delta = \sqrt{2\gamma/\pi} M$ Kn. It must be emphasized that the definition of dimensionless variables and parameters is not unique in general and the present set of definition is selected after carefully taking into consideration the well-posedness of the boundary value problem. It will be shown that the force dimensionless number ε_h (or $\varepsilon_{h_w} = \varepsilon_h/T_w^*$) is the primary factor in determining the velocity and temperature profiles across the slab. Furthermore, with average quantities u_r and T_r defined as

$$u_r = \frac{2}{h}\int_0^{h/2} u dy, \quad T_r = \frac{h/2}{\int_0^{h/2} T^{-1} dy}, \tag{3.16}$$

and with the introduction of a new variable s defined by

$$T ds = dy \quad \text{or} \quad T^* ds^* = dy^*, \tag{3.17}$$

in dimensionless form, where $s^* = sT_r/h$,

the following auxiliary relations can be derived:

$$s^*\left(y^* = \frac{1}{2}\right) = \frac{1}{2}, \quad \int_0^{1/2} u^* T^* ds^* = \frac{1}{2}, \quad \int_0^{1/2} T^* ds^* = \frac{1}{2}. \tag{3.18}$$

The relations given in Eqs. (3.15)–(3.18) represent the essence of the new method. The system of ordinary differential equations with dependent variables u and T may first be solved in terms of the variable s and the solutions are later expressed as a function of the distance y. The x-momentum equation together with the equation of state, $p=\rho RT$ and $p=p_m$, is then reduced as follows:

$$\frac{d\Pi_{xy}^*}{ds^*} = \frac{\varepsilon_h}{N_\delta} \quad \text{or} \quad \Pi_{xy}^* = \frac{\varepsilon_h}{N_\delta} s^*. \tag{3.19}$$

Here, the local thermal equilibrium condition owing to the continuous symmetric nature of conserved variables at the centerline has been applied: $\Pi_{xy}^*(0)=0$. With the assumption of Maxwell molecules, that is, $\eta(T) = \eta_w T/T_w$, the Navier–Stokes law in Eq. (3.1) can be written as

$$\Pi_{xy}^* = -\frac{1}{T_w^*}\frac{du^*}{ds^*}. \tag{3.20}$$

The velocity profile is then determined as follows:

$$u^*(s^*) = u^*(0) - T_w^*\frac{\varepsilon_h}{N_\delta}\frac{s^{*2}}{2}. \tag{3.21}$$

With the slip velocity condition,

$$u^*(s^* = 1/2) = (1-\alpha_V)u^*(s^*=0), \tag{3.22}$$

the resulting velocity profile can be expressed as

$$u^*(s^*) = u^*(0)(1-4\alpha_V s^{*2}) \quad \text{and} \quad \frac{T_w^*}{8}\frac{\varepsilon_h}{N_\delta} = \alpha_V u^*(0). \tag{3.23}$$

With the assumption of Maxwell molecules for the viscosity again, the energy equation is reduced to

$$\frac{dQ_y^*}{ds^*} = \mathrm{Pr}\ \mathrm{Ec}\ T_w^* \Pi_{xy}^{*2}. \tag{3.24}$$

When it is combined with Eq. (3.19) and is integrated once with respect to s^*, the heat flux in the y-direction can be written as

$$Q_y^* = \frac{1}{3}\mathrm{Pr}\ \mathrm{Ec}\ T_w^*\frac{\varepsilon_h^2}{N_\delta^2}s^{*3} \quad \text{or} \quad \frac{Q_y}{hp^2(0)/\eta_w} = \frac{1}{3}T_w^*\varepsilon_h^2 s^{*3}. \tag{3.25}$$

Here, again the local thermal equilibrium condition at the centerline has been applied: $Q_y^*(0)=0$. When it is combined with the Fourier law and the assumption of Maxwell

molecules for the thermal conductivity and is integrated once with respect to s^*, the following temperature profile can be determined:

$$T^*(s^*) = T^*(0) - \frac{(\gamma-1)\mathrm{Pr}\ T_w^{*3} M^2 \varepsilon_h^2}{12 N_\delta^2} s^{*4}. \tag{3.26}$$

With the dimensionless temperature jump at the wall surface in the Langmuir model defined as

$$T^*(s^* = 1/2) = \alpha_T T_w^* + (1-\alpha_T) T^*(s^* = 0), \tag{3.27}$$

the temperature profile can be expressed as ($N_\delta = \sqrt{2\gamma/\pi} M\ \mathrm{Kn}$),

$$T^*(s^*) = T^*(0) - 16\alpha_T [T^*(0) - T_w^*] s^{*4} \tag{3.28}$$

$$\text{and} \quad \frac{\pi(\gamma-1)\mathrm{Pr}\ \varepsilon_h^2 T_w^{*3}}{384\gamma\ \mathrm{Kn}^2} = \alpha_T [T^*(0) - T_w^*].$$

The centerline temperature is then calculated by using the third equation in the auxiliary relation (3.18),

$$T^*(0) = \frac{5 - \alpha_T T_w^*}{5 - \alpha_T}. \tag{3.29}$$

The temperature T_w^* can be determined by combining it with Eq. (3.28),

$$\frac{(5-\alpha_T)}{5\alpha_T} \frac{\pi(\gamma-1)\mathrm{Pr}\ \varepsilon_{h_w}^2}{384\gamma\ \mathrm{Kn}^2} T_w^{*5} + T_w^* - 1 = 0. \tag{3.30}$$

Notice that the resulting equation is now of degree 5 in stark contrast to the incompressible case [degree 1 in Eq. (3.11)]. This algebraic equation of odd degree 5 with real coefficients has always a non-negative real root and the average temperature T_w^* can be easily determined in terms of Kn and ε_{h_w} by a simple method such as the bisection method. Similar to the case of temperature, together with Eq. (3.29), the centerline velocity can be determined from the second equation in the auxiliary relation (3.18),

$$u^*(0) = \frac{21(5-\alpha_T)}{(15 - 8T_w^*)\alpha_V \alpha_T - 7(5\alpha_V + 3\alpha_T) + 105}. \tag{3.31}$$

Notice that the centerline velocity $u^*(0)$ depends now on the average temperature T_w^*, which is not the case in the incompressible case (3.13). With these centerline values, the slip velocity and the temperature jump can be determined from Eqs. (3.22) and (3.27), respectively. From the equation of state, the density profile and the average density can also be determined as

$$\rho^*(s^*) \equiv \frac{\rho}{\rho(0)} = T^*(0)\frac{p^*}{T^*} \tag{3.32}$$

$$\text{and} \quad \rho_r \equiv \frac{\int_0^{h/2} \rho dy}{h/2} = \rho(0) T^*(0).$$

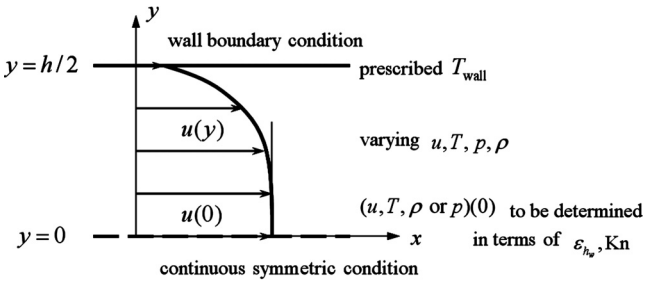

FIG. 2. Computational domain in the force-driven compressible Poiseuille gas flow.

Furthermore, the mass flow rate can be expressed as

$$\frac{\dot{m}/2h}{\rho_r\sqrt{\gamma R T_w}} \equiv \frac{\int_0^{h/2}\rho u dy}{2\sqrt{\gamma R T_w}\int_0^{h/2}\rho dy} = \frac{\sqrt{\pi}}{16\sqrt{2\gamma}} \frac{T_w^{*2}}{u^*(0)} \frac{\varepsilon_{h_w}}{\mathrm{Kn}} \frac{(1-\alpha_V/3)}{\alpha_V}. \tag{3.33}$$

Finally, through Eq. (3.17), that is, $y^* = \int_0^{s^*} T^*(s^*) ds^*$, all solutions can be transformed into the domain of the distance from the wall surface y^*,

$$y^* = s^*[5 - \alpha_T T_w^* - 16\alpha_T(1 - T_w^*)s^{*4}]/(5-\alpha_T). \tag{3.34}$$

The relation $y^* \approx s^*$, as an approximation, may be used for mathematical simplicity. An instructive relation can be further derived,

$$\left.\frac{dy^*}{ds^*}\right]_{s^*=1/2} = \frac{5 - \alpha_T(5 - 4T_w^*)}{5-\alpha_T} = \alpha_T T_w^* + (1-\alpha_T) T^*(0) = T^*(s^* = 1/2). \tag{3.35}$$

IV. NONCLASSICAL THEORY BASED ON THE NCCR MODEL

Through the pure one-dimensional assumption of $v = w = 0$, $\partial/\partial x = \partial/\partial z = 0$, the governing equation, the conservation law (2.2) and the NCCR model (2.10), is reduced to the following system of four differential and nine algebraic equations comprised of the conservation laws and constitutive equations of the shear and normal stresses and the tangential and normal heat fluxes:

$$\frac{d}{dy}\begin{bmatrix}\Pi_{xy}\\ p+\Pi_{yy}\\ \Pi_{yz}\\ \Pi_{xy}u+Q_y\end{bmatrix}=\begin{bmatrix}\rho a\\ 0\\ 0\\ \rho a u\end{bmatrix},$$

$$\begin{bmatrix}0\\0\\0\\0\\0\\0\end{bmatrix}=\frac{1}{\eta}\begin{bmatrix}(4/3)[\Pi_{xy}]_0[\Pi_{xy_0}]_0\\ -(2/3)[\Pi_{xy}]_0[\Pi_{xy_0}]_0\\ -(2/3)[\Pi_{xy}]_0[\Pi_{xy_0}]_0\\ (p+[\Pi_{yy}]_0)[\Pi_{xy_0}]_0\\ [\Pi_{yz}]_0[\Pi_{xy_0}]_0\\ 0\end{bmatrix}-\frac{p}{\eta}\begin{bmatrix}[\Pi_{xx}]_0\\ [\Pi_{yy}]_0\\ [\Pi_{zz}]_0\\ [\Pi_{xy}]_0\\ [\Pi_{xz}]_0\\ [\Pi_{yz}]_0\end{bmatrix}F(p,T,\mathbf{\Pi},\mathbf{Q},\ldots), \tag{4.1}$$

$$\begin{bmatrix}0\\0\\0\end{bmatrix}=\frac{C_p}{k}\begin{bmatrix}[\Pi_{xy}]_0[Q_{y_0}]_0+[Q_y]_0[\Pi_{xy_0}]_0/\mathrm{Pr}+a[\Pi_{xx}]_0k/C_p\\ (p+[\Pi_{yy}]_0)[Q_{y_0}]_0+a[\Pi_{xy}]_0k/C_p\\ [\Pi_{yz}]_0[Q_{y_0}]_0+a[\Pi_{xz}]_0k/C_p\end{bmatrix}-\frac{pC_p}{k}\begin{bmatrix}[Q_x]_0\\ [Q_y]_0\\ [Q_z]_0\end{bmatrix}F(p,T,\mathbf{\Pi},\mathbf{Q},\ldots).$$

Here, the dissipation terms are approximated as shear stress and heat flux multiplied by a general function of conserved and nonconserved variables, that is, $\mathbf{\Lambda}^{(\Pi)}=-p\mathbf{\Pi}F(p,T,\mathbf{\Pi},\mathbf{Q},\ldots)/\eta$ and $\mathbf{\Lambda}^{(Q)}=-pC_p\mathbf{Q}F(p,T,\mathbf{\Pi},\mathbf{Q},\ldots)/k$. Also, the constitutive relations are expressed in terms of nonconserved variables measured from its value at the center since their values may remain finite even when thermodynamic driving forces Π_{xy_0} and Q_{y_0} vanish. An abbreviation $[A]_0\equiv A-A(0)$ is introduced to represent the value of a quantity A measured from its value at the center, that is, $A(0)$.

Even though this system looks messy, it nonetheless can be solved analytically with only a few simple assumptions. Let us consider the computational domain $0\le y\le h/2$ bounded by external boundary condition at the wall and symmetric condition at the center as described in Fig. 2. From the constitutive relations, it can be identified that

$$[\Pi_{yz}]_0=[\Pi_{xz}]_0=[Q_z]_0=0, \tag{4.2}$$

$$[\Pi_{yy}]_0=[\Pi_{zz}]_0=-[\Pi_{xx}]_0/2, \tag{4.3}$$

which satisfies a physical consistency condition $[\Pi_{xx}]_0+[\Pi_{yy}]_0+[\Pi_{zz}]_0=0$. In addition, it can be noticed that the thermodynamic driving forces in the system are the velocity and temperature gradients, Π_{xy_0} and Q_{y_0}, which are defined in Eq. (2.11), that is, the Navier–Stokes–Fourier relations; the dependent variables are $p,\Pi_{yy},\Pi_{xy},u,Q_y,T$, and Q_x in order of appearance in the solutions. With these in mind, let us first consider the y-momentum equation in the conservation laws, $d(p+\Pi_{yy})/dy=0$. When it is integrated once with respect to y, the equation can be expressed as

$$p+\Pi_{yy}=p_m+\Pi_{yy}(0)\quad\text{or}\quad p+[\Pi_{yy}]_0=p_m. \tag{4.4}$$

On the other hand, when the factor $F(p,T,\mathbf{\Pi},\mathbf{Q},\ldots)$ and the driving force $[\Pi_{xy_0}]_0$ are eliminated from the constitutive equations of Π_{xy} and Π_{yy} in Eq. (4.1),

$$p[\Pi_{xy}]_0F(p,T,\mathbf{\Pi},\mathbf{Q},\ldots)=(p+[\Pi_{yy}]_0)[\Pi_{xy_0}]_0,$$

$$p[\Pi_{yy}]_0F(p,T,\mathbf{\Pi},\mathbf{Q},\ldots)=-\tfrac{2}{3}[\Pi_{xy}]_0[\Pi_{xy_0}]_0,$$

there exists a constraint on the shear and normal stresses, implying their interdependence,

$$[\Pi_{xy}]_0^2=-\tfrac{3}{2}(p+[\Pi_{yy}]_0)[\Pi_{yy}]_0. \tag{4.5}$$

Note that the factor $F(p,T,\mathbf{\Pi},\mathbf{Q},\ldots)$ is canceled out in the process, indicating no role in the qualitative behavior of the kinematic constraint. Equation (4.5), together with Eq. (4.4), is then reduced to a very instructive form for $(0\le y\le h/2)$,

$$\frac{[\Pi_{xy}]_0}{p_m}=\mathrm{sign}(\Pi_{xy_0})\sqrt{\frac{3}{2}\left(\frac{p}{p_m}-1\right)}. \tag{4.6}$$

The x-momentum equation $d\Pi_{xy}/dy=\rho a$ or $Td\Pi_{xy}/dy=ap/R$, in conjunction with the equation of state, $p=\rho RT$, is then reduced as follows to an ordinary differential equation of the pressure, in dimensionless form introduced in Eq. (3.15):

$$\frac{d\Pi_{xy}^*}{ds^*}=\frac{\varepsilon_h}{N_\delta}p^*$$
$$\text{or}\quad \frac{1}{p^*}d\left[\mathrm{sign}(\Pi_{xy_0})\sqrt{\frac{3}{2}(p^*-1)}\right]=\varepsilon_h ds^*. \tag{4.7}$$

By using an integral formula,

$$\int\frac{1}{p^*}d(\sqrt{p^*-1})=\tan^{-1}\sqrt{p^*-1}, \tag{4.8}$$

the differential equation yields the following analytical solution for the pressure and the stresses $(-h/2\le y\le h/2)$:

$$p^*(S^*) = 1 + \tan^2 S^*, \quad [\Pi^*_{yy}(S^*)]_0 = -\frac{1}{N_\delta}\tan^2 S^*,$$
$$[\Pi^*_{xy}(S^*)]_0 = \frac{1}{N_\delta}\sqrt{\frac{3}{2}}\tan S^*, \tag{4.9}$$

where

$$S^* \equiv \sqrt{2/3}\varepsilon_h s^*, \quad Y^* \equiv \sqrt{2/3}\varepsilon_h y^*.$$

Since the closure relation (2.7) is the only major assumption introduced in deriving these solutions, the tangentlike functional form and the central minimum in pressure identified from the new analytical solution of pressure and stress are believed to be universal, rather than exceptional, holding for any monatomic gases. In particular, no approximations are made for the specific forms of the factor $F(p,T,\mathbf{\Pi},\mathbf{Q},\ldots)$ in the dissipation terms. Note also that the slip (jump) boundary conditions play an indirect role at negligible levels in the solution of the pressure and stresses, only through the determination of average temperature T^*_w.

Now let us introduce an assumption for the factor $F(p,T,\mathbf{\Pi},\mathbf{Q},\ldots)$ appearing in the dissipation terms. The role of such factor in the present velocity shear flow turns out to be negligible, as observed first from its absence in the stress constraint (4.5) due to cancellation. In fact, it was shown in the previous work[28] that the exact form of the factor does not very much affect the constitutive relations of stresses in the case of the velocity shear flow. However, it is also possible that the nonlinear factor may play a non-negligible role in the case of very high Knudsen number flows. In this study, largely motivated by the advantage of analytical approach, an approximation $F(p,T,\mathbf{\Pi},\mathbf{Q},\ldots)\approx 1$, which is equivalent to the so-called relaxation time approximation (also known as the BGK approximation in literature[34]), is employed. Then, the original implicit constitutive relation (4.1) can be changed into the *explicit* relations,

$$\begin{bmatrix}0\\0\\0\\0\\0\\0\end{bmatrix} = \frac{1}{\eta}\begin{bmatrix}(4/3)[\Pi_{xy}]_0[\Pi_{xy_0}]_0\\ -(2/3)[\Pi_{xy}]_0[\Pi_{xy_0}]_0\\ -(2/3)[\Pi_{xy}]_0[\Pi_{xy_0}]_0\\ (p+[\Pi_{yy}]_0)[\Pi_{xy_0}]_0\\ [\Pi_{yz}]_0[\Pi_{xy_0}]_0\\ 0\end{bmatrix} - \frac{p}{\eta}\begin{bmatrix}[\Pi_{xx}]_0\\ [\Pi_{yy}]_0\\ [\Pi_{zz}]_0\\ [\Pi_{xy}]_0\\ [\Pi_{xz}]_0\\ [\Pi_{yz}]_0\end{bmatrix},$$
$$\begin{bmatrix}0\\0\\0\end{bmatrix} = \frac{C_p}{k}\begin{bmatrix}[\Pi_{xy}]_0[Q_{y_0}]_0 + [Q_y]_0[\Pi_{xy_0}]_0/\mathrm{Pr} + a[\Pi_{xx}]_0 k/C_p\\ (p+[\Pi_{yy}]_0)[Q_{y_0}]_0 + a[\Pi_{xy}]_0 k/C_p\\ [\Pi_{yz}]_0[Q_{y_0}]_0 + a[\Pi_{xz}]_0 k/C_p\end{bmatrix} - \frac{pC_p}{k}\begin{bmatrix}[Q_x]_0\\ [Q_y]_0\\ [Q_z]_0\end{bmatrix}. \tag{4.10}$$

Here, it must be emphasized that the following solutions (profiles of velocity, temperature or density, and heat flux) will be valid only within the limitation of the relaxation [or Bhatnagar–Gross–Krook (BGK)] approximation $F(p,T,\mathbf{\Pi},\mathbf{Q},\ldots)=1$. Then there exists a simple relation in the constitutive relation of stresses

$$p[\Pi_{xy}]_0 = p_m[\Pi_{xy_0}]_0. \tag{4.11}$$

With the assumption of Maxwell molecules and the definition of Π_{xy_0}, Eq. (4.11) is then reduced to

$$[\Pi^*_{xy}]_0 = -\frac{1}{p^* T^*_w}\frac{du^*}{ds^*}. \tag{4.12}$$

By following the same procedure developed in Sec. III B of classical theory based on the compressible Navier–Stokes–Fourier relations, the following velocity profile can be derived ($S^*_{1/2} \equiv \sqrt{2/3}\varepsilon_h \cdot 0.5$),

$$u^*(S^*) = u^*(0)\left[1 - 4\alpha_V\left(\frac{\tan S^*}{2\tan S^*_{1/2}}\right)^2\right]$$
$$\text{and} \quad \frac{T^*_w \varepsilon_h}{8N_\delta}\left(\frac{\tan S^*_{1/2}}{S^*_{1/2}}\right)^2 = \alpha_V u^*(0). \tag{4.13}$$

In contrast to the classical case, the pressure distribution is not uniform and the wall pressure appearing in the fraction of the wall surface covered at thermal equilibrium $\alpha_V = \bar{\beta}_V p^*_w/(1+\bar{\beta}_V p^*_w)$ may be expressed as $p^*_w = 1+\tan^2 S^*_{1/2}$. In addition, similar to the previous case of classical theory, the energy equation and the normal heat flux in the y-direction can be expressed as

$$\frac{dQ_y^*}{ds^*} = \Pr\ \mathrm{Ec}\ T_w^* p^* [\Pi_{xy}^*]_0^2,$$

$$[Q_y^*]_0 = \frac{1}{3}\Pr\ \mathrm{Ec}\ T_w^* \frac{\varepsilon_h^2}{N_\delta^2}\left(\frac{\tan S^*}{2S_{1/2}^*}\right)^3 \tag{4.14}$$

$$\text{or}\quad \frac{[Q_y]_0}{hp^2(0)/\eta_w} = \frac{T_w^*\varepsilon_h^2}{3}\left(\frac{\tan S^*}{2S_{1/2}^*}\right)^3.$$

However, the determination of the temperature profile becomes far more complicated than that in the classical theory, owing to the non-Fourier law arising in the constitutive relations of heat flux. When the constitutive relation of Q_y in Eq. (4.1) is combined first with Eq. (4.4) and then with the assumption of Maxwell molecules and the definition of Q_{y_0} in Eq. (2.11), the resulting equation can be written as

$$\frac{dT^*}{ds^*} + m(s^*)T^* = n(s^*), \tag{4.15}$$

where

$$m(s^*) \equiv -\frac{(\gamma-1)}{\gamma} N_\delta \varepsilon_h [\Pi_{xy}^*]_0,$$

$$n(s^*) \equiv -\frac{\Delta T}{T_r} p^* [Q_y^*]_0 T_w^*.$$

Owing to the second term on the left-hand side, it is now a (linear) differential equation of Bernoulli type and the general solution can be written as

$$T^*(s^*) = e^{-\int m(s^*)ds^*}\left[\int e^{\int m(s^*)ds^*} n(s^*)ds^* + \text{const}\right]. \tag{4.16}$$

After combining it with Eqs. (4.9) and (4.14) and an integral formula,

$$\int \frac{\sin^3 s^*}{\cos^{5-e} s^*} ds^* = \frac{1}{(4-e)\cos^{4-e} s^*} - \frac{1}{(2-e)\cos^{2-e} s^*}, \tag{4.17}$$

the solution can be expressed as, in a compact form,

$$T^*(S^*) = \sec^e S^*\left[T^*(0) - \frac{(\gamma-1)\Pr\ T_w^{*3} M^2 \varepsilon_h^2}{192 N_\delta^2 (1-e/4)} \frac{F(S^*)}{S_{1/2}^{*4}}\right], \tag{4.18}$$

where the function $F(S^*)$ is defined as

$$F(S^*) \equiv (4-e)\left[\frac{1}{(4-e)\cos^{4-e} S^*} - \frac{1}{(2-e)\cos^{2-e} S^*} - \left(\frac{1}{4-e} - \frac{1}{2-e}\right)\right], \quad e = \frac{3(\gamma-1)}{2\gamma}.$$

The factor $\sec^e S^*$ is directly related to the number ε_h since it is derived from $e^{-\int m(s^*)ds^*}$. It is positive and increases with regard to the distance y and it can be expanded as

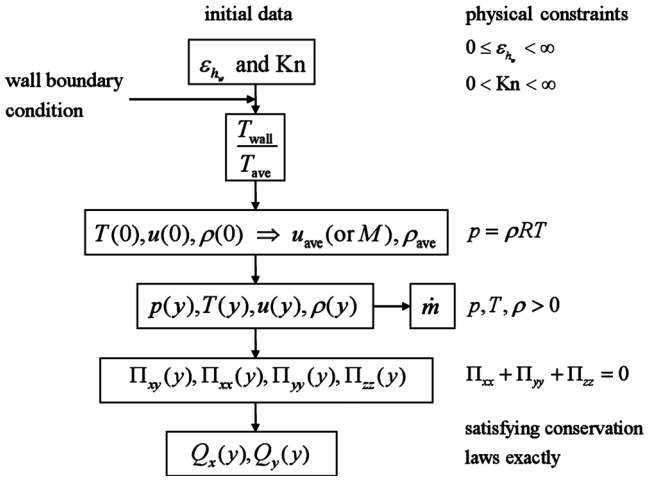

FIG. 3. Diagram of unique flow solution for the force-driven compressible Poiseuille gas flow for the given condition.

$$\sec^e S^* = 1 + \frac{e}{2}S^{*2} + O(S^{*4}).$$

The function $F(S^*)$ is positive and monotonic since the first nonzero derivative $F^{(iv)}(S^*=0) = 24-6e$ is positive. The following power series shows its role very similar to the quartic function in the Navier–Stokes–Fourier solution (3.28),

$$F(S^*) = (1-e/4)S^{*4} + O(S^{*6}).$$

With the temperature jump at the wall surface (3.27), the temperature profile can be determined as follows:

$$T^*(S^*) = \sec^e S^*\left\{T^*(0) - \{T^*(0) - \sec^{-e} S_{1/2}^* \times [\alpha_T T_w^* + (1-\alpha_T)T^*(0)]\}\frac{F(S^*)}{F(S_{1/2}^*)}\right\}, \tag{4.19}$$

$$\frac{\pi(\gamma-1)\Pr\ \varepsilon_{h_w}^2 T_w^{*5}}{384\gamma\ \mathrm{Kn}^2(1-e/4)}\frac{F(S_{1/2}^*)}{S_{1/2}^{*4}} = T^*(0)[1-(1-\alpha_T)\sec^{-e} S_{1/2}^*] - \alpha_T T_w^* \sec^{-e} S_{1/2}^*.$$

Similar to the classical case, the equation is reduced to the algebraic equation of odd degree 5 with real coefficients. The unknown value T_w^* for given values of Kn and ε_{h_w} can be determined uniquely by using the bisection method in which an upper limit of T_w^* may be given as $\sqrt{3/2}\pi/\varepsilon_{h_w}$ $(S_{1/2}^* \to \pi/2)$. In addition, the auxiliary relation (3.18) and Eq. (3.17) yield, in the present nonclassical case,

$$T^*(0) = \frac{S_{1/2}^* F(S_{1/2}^*) - \sec^{-e} S_{1/2}^*[\alpha_T T_w^* + (1-\alpha_T)T^*(0)]G(S_{1/2}^*)}{F(S_{1/2}^*)H(S_{1/2}^*) - G(S_{1/2}^*)},$$

or

$$T^*(0)=\frac{S^*_{1/2}F(S^*_{1/2})-\alpha_T G(S^*_{1/2})T^*_w \sec^{-e} S^*_{1/2}}{F(S^*_{1/2})H(S^*_{1/2})-G(S^*_{1/2})+(1-\alpha_T)G(S^*_{1/2})\sec^{-e} S^*_{1/2}}, \tag{4.20}$$

$$u^*(0)=S^*_{1/2}F(S^*_{1/2})\tan^2 S^*_{1/2}\{\alpha_T T^*_w \sec^{-e} S^*_{1/2}[G(S^*_{1/2})\tan^2 S^*_{1/2}-\alpha_V I(S^*_{1/2})]+T^*(0)\{\tan^2 S^*_{1/2}[F(S^*_{1/2})H(S^*_{1/2})-G(S^*_{1/2})] + \alpha_V[I(S^*_{1/2})-F(S^*_{1/2})J(S^*_{1/2})]+(1-\alpha_T)\sec^{-e} S^*_{1/2}[G(S^*_{1/2})\tan^2 S^*_{1/2}-\alpha_V I(S^*_{1/2})]\}\}^{-1}, \tag{4.21}$$

$$Y^*(S^*)=T^*(0)H(S^*)+G(S^*) \times\{[\alpha_T T^*_w+(1-\alpha_T)T^*(0)]\sec^{-e} S^*_{1/2} - T^*(0)\}/F(S^*_{1/2}), \tag{4.22}$$

where

$$G(S^*)\equiv\int F(S^*)\sec^e S^* dS^* = \frac{1}{3}\tan^3 S^*+\frac{2}{(2-e)}[H(S^*)-\tan S^*],$$

$$H(S^*)\equiv\int \sec^e S^* dS^*, \tag{4.23}$$

$$I(S^*)\equiv\int F(S^*)\tan^2 S^* \sec^e S^* dS^* = \frac{1}{5}\tan^5 S^*+\frac{2}{(2-e)}\left[J(S^*)-\frac{1}{3}\tan^3 S^*\right],$$

$$J(S^*)\equiv\int \tan^2 S^* \sec^e S^* dS^* = \frac{1}{1+e}[\tan S^* \sec^e S^*-H(S^*)].$$

In the expressions, $H(S^*)$ is the essential element that requires a numerical integration method such as the Simpson's rule. The slope of Y^* in S^* can be determined by

$$\left.\frac{dY^*}{dS^*}\right]_{S^*_{1/2}}=\alpha_T T^*_w+(1-\alpha_T)T^*(0)=T^*(S^*_{1/2}). \tag{4.24}$$

Now the density profile and the average density can be expressed as

$$\rho^*(s^*)=T^*(0)\frac{p^*}{T^*} \quad \text{and} \quad \rho_r=\rho(0)T^*(0). \tag{4.25}$$

The tangential heat flux Q_x can be determined afterward from the constitutive relation of Q_x in Eq. (4.1) and $[\Pi_{xx}]_0=-2[\Pi_{yy}]_0$ in the relation (4.3). The tangential heat flux can be written as follows:

$$[Q^*_x]_0=N_\delta\left[\left(1+\frac{1}{\mathrm{Pr}}\right)[\Pi^*_{xy}]_0[Q^*_y]_0-\frac{\varepsilon_h}{T^*_w}\frac{T_r}{\Delta T}\frac{(\gamma-1)}{\gamma}\frac{T^*}{p^*}(2[\Pi^*_{yy}]_0+N_\delta[\Pi^*_{xy}]^2_0)\right] \tag{4.26}$$

$$\text{or} \quad \frac{[Q_x]_0}{hp^2(0)/\eta_w}=\frac{\varepsilon_h^3}{T^{*2}_w}\left(\frac{\tan S^*}{2S^*_{1/2}}\right)^2\left[\left(1+\frac{1}{\mathrm{Pr}}\right)\frac{T^{*3}_w}{3}\left(\frac{\tan S^*}{2S^*_{1/2}}\right)^2+\frac{2}{3\pi}\frac{\mathrm{Kn}^2}{\mathrm{Pr}}\frac{T^*}{p^*}\right].$$

Finally, the mass flow rate can be expressed as

$$\frac{\dot m/2h}{\rho_r\sqrt{\gamma RT_w}}=\frac{\sqrt{\pi}}{16\sqrt{2}\gamma}\frac{T^{*2}_w}{u^*(0)}\frac{\varepsilon_{h_w}}{\mathrm{Kn}}\frac{(1-\alpha_V/3)}{\alpha_V}\left(\frac{\tan S^*_{1/2}}{2S^*_{1/2}}\right)^2. \tag{4.27}$$

A diagram given in Fig. 3 explains how a unique flow solution can be constructed for a given set of physical condition specified in terms of the dimensionless number ε_{h_w} and the Knudsen number. Table I also summarizes classical (incompressible and compressible) Navier–Stokes–Fourier and nonclassical NCCR solutions.

V. RESULTS AND DISCUSSION

Equations (4.2)–(4.27) represent a complete set of fully analytical solution obtained by a nonclassical theory based on the NCCR model. In addition, Eqs. (3.19)–(3.35) represent complete analytical solution of the compressible Navier–Stokes–Fourier theory. In both cases, the temperature dependence of viscosity and thermal conductivity is treated in a mathematically rigorous way by developing a new technique [Eqs. (3.15)–(3.18)]. By doing so, the existence of analytical solution for the physical conditions ($0\le\varepsilon_{h_w}<\infty$ and $0<\mathrm{Kn}<\infty$) has been shown through algebraic equations of degree 5 [Eqs. (3.30) and (4.19)].

TABLE I. Comparison of incompressible and compressible Navier–Stokes–Fourier and NCCR solutions ($S^* \equiv \sqrt{2/3}T_w^* \varepsilon_{h_w} s^*$, $s^* \equiv sT_r/h$, $Tds=dy$, $y^* \equiv y/h$, $[A]_0 \equiv A-A(0)$).

Items	Incompressible NSF	Compressible NSF (new)	NCCR (new)
$\frac{p}{p(0)}$	1	1	$1+\tan^2 S^*$; $1-\tanh^2\left(\sqrt{\frac{7}{2}}S^*\right)$ (diatomic)
$\frac{u}{u(0)}$	$1-\frac{1}{2u(0)}\cdot\frac{\rho a h^2}{\eta}y^{*2}$	$1-\frac{T_w^*}{2u^*(0)}\cdot\frac{\varepsilon_{h_w}}{N_\delta}s^{*2}$	$1-\frac{T_w^*}{2u^*(0)}\frac{\varepsilon_{h_w}}{N_\delta}\cdot\left(\frac{\tan S^*}{2S_{1/2}^*}\right)^2$
$\frac{T}{T(0)}$	$1-\frac{\rho^2 a^2 h^4}{12\eta k T(0)}y^{*4}$	$1-\frac{\pi(\gamma-1)\mathrm{Pr}}{24\gamma}\frac{T_w^{*5}}{T^*(0)}\cdot\frac{\varepsilon_{h_w}^2}{\mathrm{Kn}^2}s^{*4}$	$\sec^e S^*\left[1-\frac{\pi(\gamma-1)\mathrm{Pr}}{24\gamma(1-e/4)}\frac{T_w^{*5}}{T^*(0)}\cdot\frac{\varepsilon_{h_w}^2}{\mathrm{Kn}^2}\frac{F(S^*)}{(2S_{1/2}^*)^4}\right]$
$\frac{[\Pi_{xy}]_0}{p(0)}$	$\frac{\rho a h}{p(0)}y^*$	$T_w^*\varepsilon_{h_w}s^*$	$\sqrt{\frac{3}{2}}\tan S^*$; $\sqrt{\frac{3}{7}}\tanh\left(\sqrt{\frac{7}{2}}S^*\right)$ (diatomic)
$\frac{[\Pi_{yy}]_0}{p(0)}$	0	0	$-\tan^2 S^*$; $-\frac{2}{7}\tanh^2\left(\sqrt{\frac{7}{2}}S^*\right)$ (diatomic)
$\frac{[Q_y]_0}{hp^2(0)/\eta_w}$	$\frac{1}{3}\left(\frac{\rho a h}{p(0)}\right)^2 y^{*3}$	$\frac{1}{3}T_w^{*3}\varepsilon_{h_w}^2 s^{*3}$	$\frac{1}{3}T_w^{*3}\varepsilon_{h_w}^2\left(\frac{\tan S^*}{2S_{1/2}^*}\right)^3$
$\frac{[Q_x]_0}{hp^2(0)/\eta_w}$	0	0	$\varepsilon_{h_w}^3 T_w^*\left(\frac{\tan S^*}{2S_{1/2}^*}\right)^2\left[\left(1+\frac{1}{\mathrm{Pr}}\right)\frac{T_w^{*3}}{3}\cdot\left(\frac{\tan S^*}{2S_{1/2}^*}\right)^2+\frac{2}{3\pi}\frac{\mathrm{Kn}^2}{\mathrm{Pr}}\frac{T^*}{p^*}\right]$
$T_w^*, u^*(0), M$	Equations (3.5), (3.11), and (3.13)	Equations (3.23), (3.30), and (3.31)	Equations (4.13), (4.19), and (4.21)
$\frac{\dot{m}/2h}{\rho_r\sqrt{\gamma R T_w}}$	$\frac{\rho a h^2}{16\eta\sqrt{\gamma R T_w}}\frac{(1-\alpha_V/3)}{\alpha_V}$	$\frac{\sqrt{\pi}}{16\sqrt{2\gamma}}\frac{T_w^{*2}}{u^*(0)}\frac{\varepsilon_{h_w}}{\mathrm{Kn}}\frac{(1-\alpha_V/3)}{\alpha_V}$	$\frac{\sqrt{\pi}}{16\sqrt{2\gamma}}\frac{T_w^{*2}}{u^*(0)}\frac{\varepsilon_{h_w}}{\mathrm{Kn}}\frac{(1-\alpha_V/3)}{\alpha_V}\left(\frac{\tan S_{1/2}^*}{2S_{1/2}^*}\right)^2$
Temperature dependence	Neglected	Exact (Maxwell) Eq. (3.34)	Exact (Maxwell) Eqs. (4.22) and (4.23)

The analytical solution, first of all, enables the underlying physics behind critical questions, the abnormal properties (nonuniform pressure and temperature minimum) in the present problem, to be identified. A close examination of Eqs. (4.4)–(4.9) reveals that the presence of nonzero normal stress predicted by the kinematic constraint on viscous stresses (4.5) is the direct cause of the nonuniform pressure distribution. The peculiar nature of the force-driven Poiseuille flow—appearance of the forcing term ρa in the x-momentum equation of the conservation laws—makes this stress constraint stand unexpectedly even in gas flows with small Knudsen numbers. The presence of the kinematic stress constraint in the velocity shear flow was discovered first by Eu.[2] Also, a detailed investigation of the constraint including diatomic gases was conducted by Myong[5–7] in which the nonlinear coupled constitutive relations were actually solved in the domain scaled by the hydrodynamic pressure; subsequently, the exact nature of the constraint was illuminated.

The existence of the central temperature minimum in the force-driven Poiseuille flow may also be explained by examining the analytical solution. For example, when the temperature solution (4.19) is examined, it is obvious that the temperature near the centerline is at a minimum owing to the factor $\sec^e S^*$; the origin of the factor is traced to the second term on the left-hand side of the differential equation (4.15). In other words, the extra coupling term of viscous shear stress and force $a\Pi_{xy}$ appearing in the non-Fourier constitutive relation of the heat flux (4.1) is the ultimate source of the central temperature minimum. It is also instructive to examine the central temperature minimum together with the normal heat flux in the y-direction given in Eq. (4.14). Since the heat flux remains positive for positive y, the central region shows a heat transfer from the cold region to the hot region, which is a very surprising result against the conventional Fourier law.[35] Furthermore, the existence of the temperature minimum can be proven without actually calculating the temperature profile by integrating the differential equation, which is summarized in Appendix B. The second derivative of the temperature profile is shown to become positive at the centerline; its magnitude is directly proportional to the force-related dimensionless number ε_h. Note that the slip boundary conditions do not play any role in the proof.

The analytical solution also illustrates how a unique flow solution is constructed from the given physical conditions. For example, a set of physical conditions a, h, T_w, p_m together with gas constants R, γ, Pr will determine the average temperature T_r first through Eq. (3.30) or Eq. (4.19) and then the average velocity u_r through Eq. (3.23) or Eq. (4.13). Since the algebraic equation (3.30) or Eq. (4.19) of odd degree 5 with real coefficients has always a non-negative real root, the new solution represented by the average tempera-

TABLE II. Examples of new analytical solutions.

$\varepsilon_{h_w}=0.3$		NCCR			Compressible NSF	
Kn	0.01	0.1	1.0	0.01	0.1	1.0
T_w^*	0.707 03	0.982 68	1.020 6	0.707 54	0.978 83	0.999 06
$T^*(0)$	1.069 1	1.002 2	0.998 48	1.069 6	1.003 5	1.0
$u^*(0)$	1.417 5	1.311 4	1.072 2	1.418 5	1.310 8	1.071 4
α_V, α_T	0.961 82	0.717 24	0.202 52	0.961 54	0.714 29	0.200 00
M	1.341 6	0.377 41	0.176 48	1.336 3	0.372 53	0.169 57
$\dot{m}/(2\rho_r h\sqrt{\gamma RT_w})$	0.455 72	0.143 59	0.082 284	0.453 98	0.141 91	0.079 135
$\varepsilon_{h_w}=0.6$		NCCR			Compressible NSF	
Kn	0.01	0.1	1.0	0.01	0.1	1.0
T_w^*	0.575 53	0.942 49	1.089 2	0.577 23	0.933 27	0.996 30
$T^*(0)$	1.099 0	1.006 9	0.993 09	1.100 7	1.011 1	1.000 2
$u^*(0)$	1.393 5	1.308 7	1.074 8	1.395 9	1.307 3	1.071 4
α_V, α_T	0.962 27	0.725 13	0.211 78	0.961 54	0.714 29	0.200 00
M	1.822 6	0.706 53	0.398 28	1.807 4	0.679 15	0.337 28
$\dot{m}/(2\rho_r h\sqrt{\gamma RT_w})$	0.619 01	0.267 88	0.185 08	0.614 05	0.258 72	0.157 40

ture T_w^* is well-defined for all Knudsen numbers and for all force-related dimensionless numbers ε_{h_w}. As described in Fig. 3, this process may be modified; information of the two dimensionless numbers ε_{h_w}, Kn and the wall temperature T_w, will determine the dimensionless parameter T_w^* (or the average temperature T_r) through Eq. (3.30) or Eq. (4.19) and later the composite number N_δ (or the average velocity u_r).

In order to compare the new solutions (compressible Navier–Stokes–Fourier and NCCR theories) with other results, a case, $\varepsilon_{h_w}=0.6$ and Kn=0.1, is considered in the present study. When the coefficient ω_V, ω_T in the Langmuir slip model is assumed to be 1, the parameter $\alpha_V=\alpha_T=1/(1+4\ \mathrm{Kn})$ is equal to 0.714 29. In these conditions, the compressible Navier–Stokes–Fourier theory yields $T_w^*=0.933\ 27$, $u^*(0)=1.3073$, and $M=0.679\ 15$, respectively, while the nonclassical NCCR theory yields $T_w^*=0.942\ 49$, $u^*(0)=1.3087$, and $M=0.706\ 53$, respectively. (Other examples are summarized in Table II.) Among various theoretical calculations, the most comprehensive DSMC result for a hard sphere gas obtained by Uribe and Garcia[20] is chosen for the comparison study. As the first result, the relation between the actual distance y^* and the distance s^* is depicted in Fig. 4. Since the slope at the centerline $dy^*/ds^*(0)=T^*(0)$ is greater than 1, the actual distance y^* is always smaller than the one predicted by assuming $y^*=s^*$, where the temperature dependence is ignored. In addition, since the difference between y^* and s^* turns out to be small, it will not affect the essence of nonuniform pressure and temperature minimum near the centerline. However, it can play a significant role in the slope of velocity profile at the wall $du^*/dy^*]_{y^*=1/2}$ in the flow with high ε_{h_w} and low Knudsen number since $dy^*/ds^*]_{s^*=1/2}$ in Eq. (3.35) or Eq. (4.24) increases considerably in such flow.

In Figs. 5–8, the conserved variables (velocity, temperature, pressure, and density) are depicted with regard to the location y^*. Indeed, the concave-shape (monotonic variation from the center to the wall) pressure and density distributions and the temperature minimum near the centerline are convincingly demonstrated by the NCCR theory. It must be mentioned that the compressible Navier–Stokes–Fourier solutions used in these figures are more accurate than the incompressible Navier–Stokes–Fourier solutions in previous works since the usual assumption of ignoring the temperature dependence of $\eta(T)$, $k(T)$, and ρ in the x-momentum equation $d\Pi_{xy}/dy=\rho a$ is removed in the analysis. The nonconserved variables (shear stress, normal stresses, normal heat flux, and tangential heat flux) measured from the values at the center are depicted with regard to the location y^* in Figs. 9–12 since we confine our interest to only qualitative behavior within the domain. The value of nonconserved variables at the center may be either taken by DSMC data in which non-negligible values at the center seem to be observed or determined by other consideration. For example, if

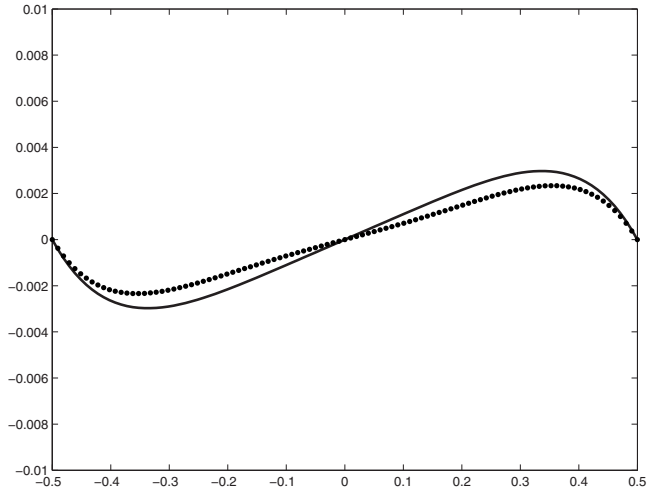

FIG. 4. The relation between the actual distance y and a distance s scaled by the local temperature distribution ($\varepsilon_{h_w}=0.6$, Kn=0.1). The horizontal axis represents the distance y^*, while the vertical axis represents the difference (y^*-s^*). The (●) symbols represent the NCCR theory, while the (–) represents the compressible Navier–Stokes–Fourier result.

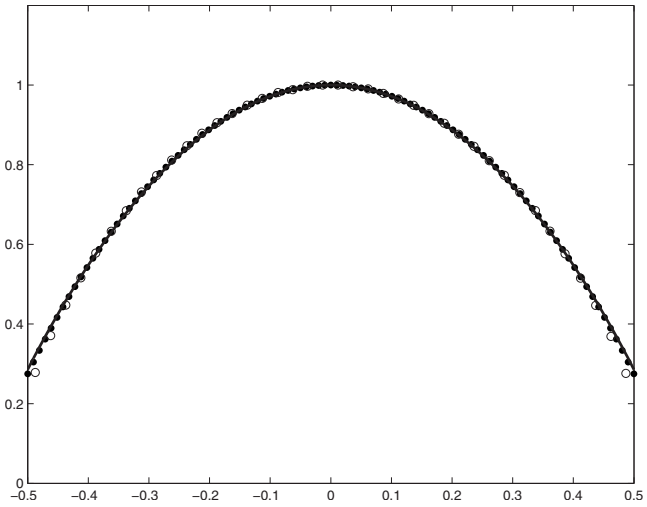

FIG. 5. Velocity distribution $u(y^*)/u(0)$ in the force-driven compressible Poiseuille gas flow ($\varepsilon_{h_w}=0.6$, Kn=0.1). The (●) and (○) symbols represent the NCCR theory and DSMC results, while the (–) represents the compressible Navier–Stokes–Fourier result.

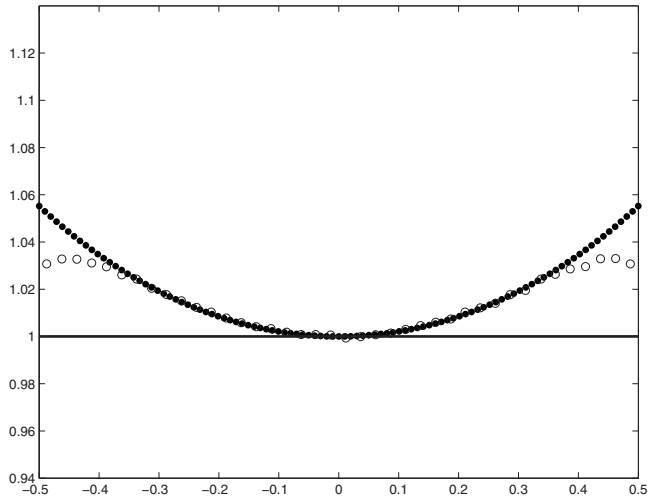

FIG. 7. Pressure distribution $p(y^*)/p(0)$ in the force-driven compressible Poiseuille gas flow ($\varepsilon_{h_w}=0.6$, Kn=0.1). The (●) and (○) symbols represent the NCCR theory and DSMC results, while the (–) represents the compressible Navier–Stokes–Fourier result.

a phenomenological interpretation described in Appendix C is applied, they will remain strictly zero. However, it would be safe to say that a definitive answer is not yet available and the further study is needed to resolve this issue. In these figures, the nonzero normal stresses and the non-negligible tangential heat flux are convincingly demonstrated by the NCCR theory. Notice also that the sign of normal stresses and heat fluxes coincides in both theories (NCCR and DSMC). In addition, both theories predict that the *xx*-component of normal stress in Fig. 10 is greater in magnitude than *zz*-component of normal stress and the tangential heat flux measured from the center in Fig. 12 remains nonnegative. In order to confirm the existence of the kinematic constraint on viscous stresses in the velocity shear flow, the normal stresses scaled by the pressure $[\Pi_{yy}]_0/p$ of NCCR and DSMC are plotted versus the linear shear stress scaled by the pressure $[\Pi_{xy}]_0/p$ in Fig. 13. It can be observed that the NCCR theory is in qualitative agreement with the DSMC prediction. Overall, the present nonclassical NCCR theory captures most of the qualitative features predicted by the DSMC calculation.

The central temperature minimum also turns out to change significantly the mechanism of the mass flow rate given in Eq. (4.27). Figure 14 shows the average temperature and velocity versus the Knudsen number for $\varepsilon_{h_w}=0.3$. It can be observed that the wall temperature scaled by the average temperature T_w^* deviates from the classical theory, while the velocity $u^*(0)$ remains very close to the classical theory. This, in turn, causes the increase of the mass flow rate around $O(\mathrm{Kn})=1$ since the mass flow rate for a given ε_{h_w} is proportional to $T_w^{*2}/[\alpha_V\ \mathrm{Kn}\ u^*(0)]$. This behavior, which is

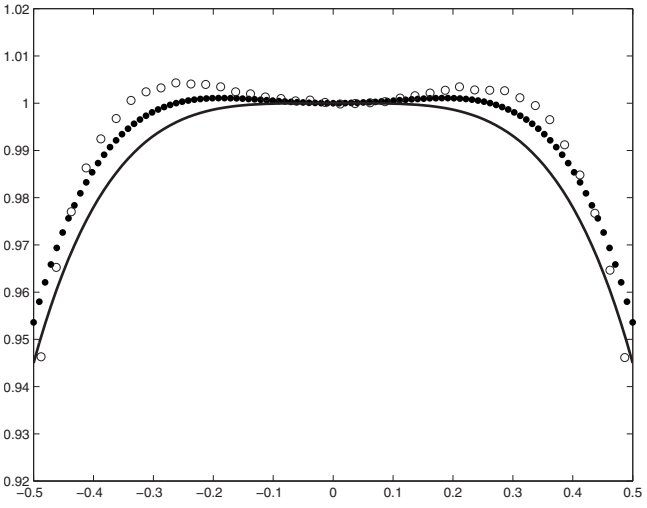

FIG. 6. Temperature distribution $T(y^*)/T(0)$ in the force-driven compressible Poiseuille gas flow ($\varepsilon_{h_w}=0.6$, Kn=0.1). The (●) and (○) symbols represent the NCCR theory and DSMC results, while the (–) represents the compressible Navier–Stokes–Fourier result.

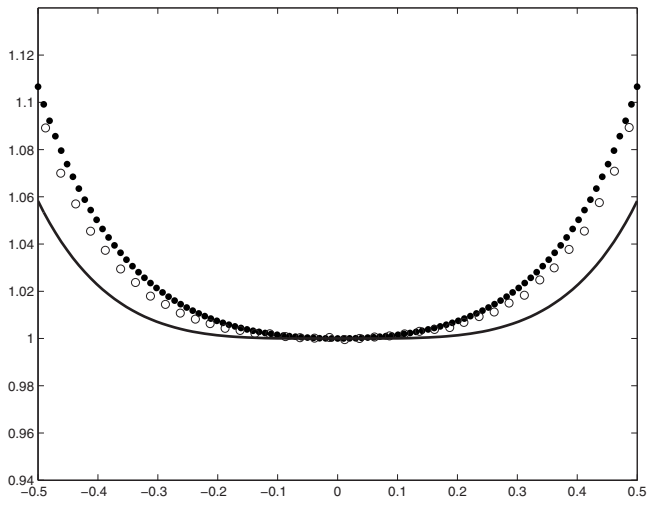

FIG. 8. Density distribution $\rho(y^*)/\rho(0)$ in the force-driven compressible Poiseuille gas flow ($\varepsilon_{h_w}=0.6$, Kn=0.1). The (●) and (○) symbols represent the NCCR theory and DSMC results, while the (–) represents the compressible Navier–Stokes–Fourier result.

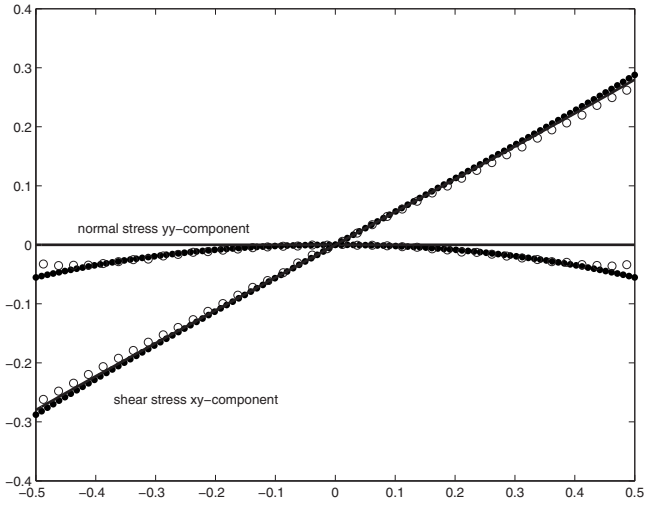

FIG. 9. Stress distribution (shear and normal $[\Pi_{xy,yy}(y^*)]_0/p(0)$) in the force-driven compressible Poiseuille gas flow ($\varepsilon_{h_w}=0.6$, Kn=0.1). The (●) and (○) symbols represent the NCCR theory and DSMC results, while the (–) represents the compressible Navier–Stokes–Fourier result.

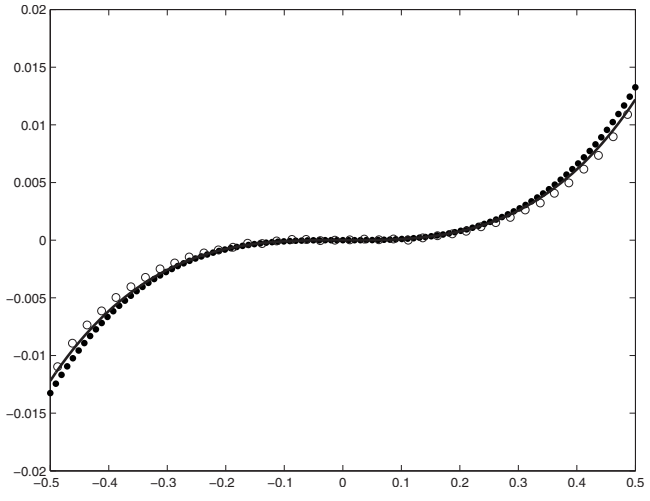

FIG. 11. Heat flux (normal $[Q_y(y^*)]_0/(hp^2(0)/\eta_w)$) distribution in the force-driven compressible Poiseuille gas flow ($\varepsilon_{h_w}=0.6$, Kn=0.1). The (●) and (○) symbols represent the NCCR theory and DSMC results, while the (–) represents the compressible Navier–Stokes–Fourier result.

demonstrated in Fig. 15, is similar to the Knudsen minimum in the case of the pressure-driven Poiseuille flow.

Finally, since the present nonclassical theory also holds for more complicated gases, the same methodology developed for monatomic gas can be carried over to diatomic gases, which is described in Appendix D. In stark contrast to monatomic case, as shown in Eq. (D13), the convex (hyperbolic tangent) pressure profile with a maximum at the center is theoretically predicted for diatomic gases. The effect of the bulk viscosity associated with rotational degrees of freedom in diatomic gases on the pressure distribution is illustrated in Fig. 16. The pressure distribution is depicted for $f_b=0.0, 2/9, 1.0$ over the distance s^*. It can be observed that the pressure profile becomes less concave as the bulk viscosity increases and across a critical point it turns into a convex shape.

VI. CONCLUDING REMARKS

A complete set of fully analytical solutions of the Navier–Stokes–Fourier and nonclassical NCCR models for the force-driven compressible Poiseuille gas flow in the case of Maxwellian molecules is presented in compact functional form. The construction of a unique flow solution for all physical conditions (expressed in terms of the Knudsen number and the force-related dimensionless number) is successfully demonstrated in the new theory. By developing a mathematical framework in which the temperature dependence of transport coefficients is taken into account in a rigorous way, the exact role of a quantity called the average temperature is also illuminated. Furthermore, in stark contrast to monatomic case, the convex pressure profile with a maximum at the

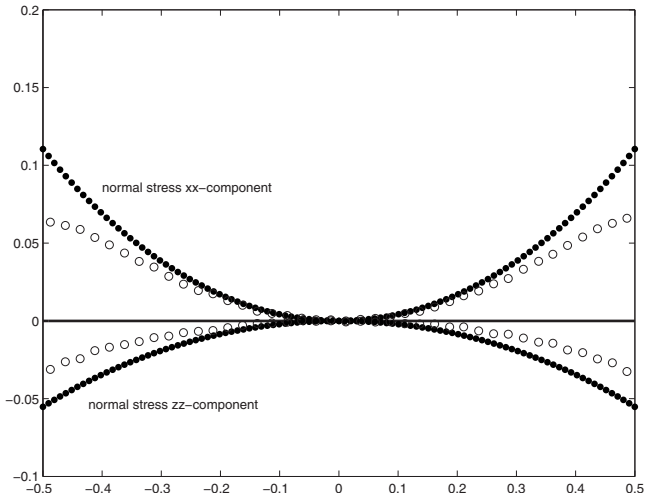

FIG. 10. Stress distribution (normal $[\Pi_{xx,zz}(y^*)]_0/p(0)$) in the force-driven compressible Poiseuille gas flow ($\varepsilon_{h_w}=0.6$, Kn=0.1). The (●) and (○) symbols represent the NCCR theory and DSMC results, while the (–) represents the compressible Navier–Stokes–Fourier result.

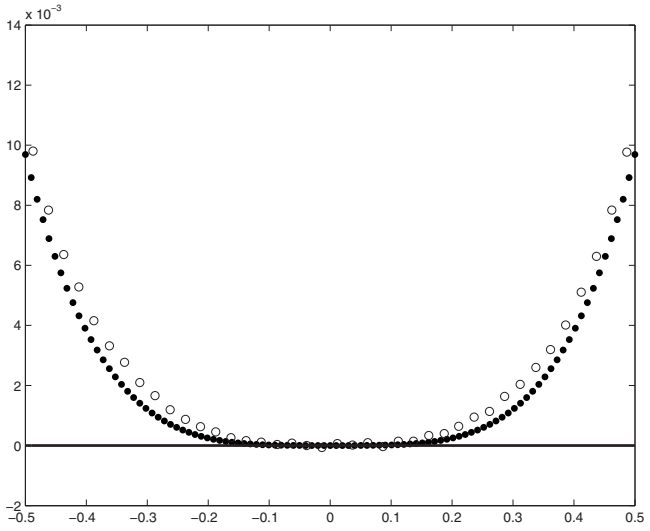

FIG. 12. Heat flux (tangential $[Q_x(y^*)]_0/(hp^2(0)/\eta_w)$) distribution in the force-driven compressible Poiseuille gas flow ($\varepsilon_{h_w}=0.6$, Kn=0.1). The (●) and (○) symbols represent the NCCR theory and DSMC results, while the (–) represents the compressible Navier–Stokes–Fourier result.

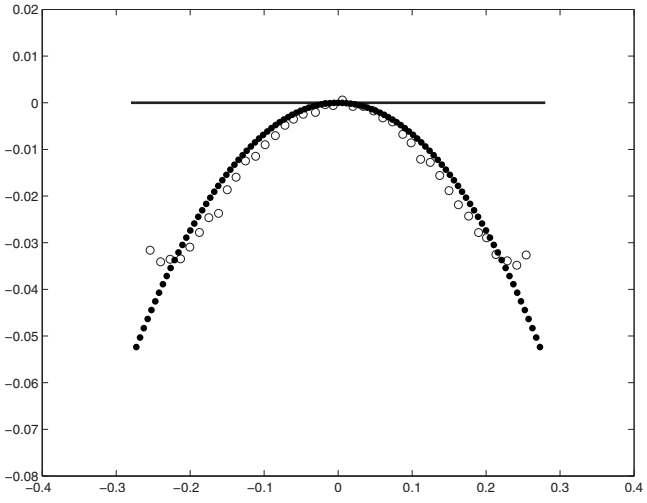

FIG. 13. Kinematic constraint on viscous stresses in the force-driven compressible Poiseuille gas flow ($\varepsilon_{h_w}=0.6$, Kn=0.1); $[\Pi_{xy}]_0/p$ vs $[\Pi_{yy}]_0/p$ for $-1/2<y^*<1/2$. The (●) and (○) symbols represent the NCCR theory and DSMC results, while the (–) represents the compressible Navier–Stokes–Fourier result.

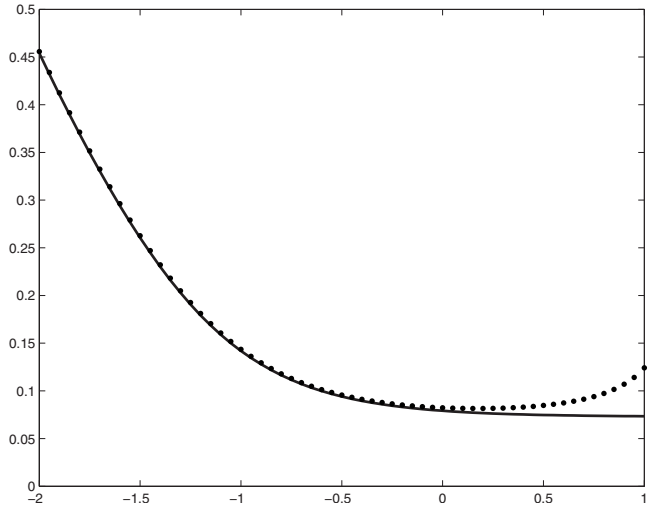

FIG. 15. Mass-flow rate $[\dot{m}/(2\rho_r h\sqrt{\gamma RT_w})]$ vs the Knudsen number in logarithmic scale in the force-driven compressible Poiseuille gas flow ($\varepsilon_{h_w}=0.3$). The (●) symbols represent the NCCR theory, while the (–) represents the compressible Navier–Stokes–Fourier result.

center is predicted for diatomic gases. A further study on this new finding will be conducted in future works.

The basic tenet used in this study consists of a mathematical technique (3.15)–(3.18) for taking into account temperature variation of viscosity and thermal conductivity coefficients and the physically motivated NCCR models (4.1) and (4.10) (non-Newtonian stress constraint, non-Fourier heat flux law). The tenet is, in principle, applicable for any other gas flows such as plane Couette flow (the Knudsen layer problem) and pressure-driven Poiseuille flow, which are other very important problems in rarefied and microscale gases. The results of the studies on these problems based on the framework developed here will also be reported in future works.

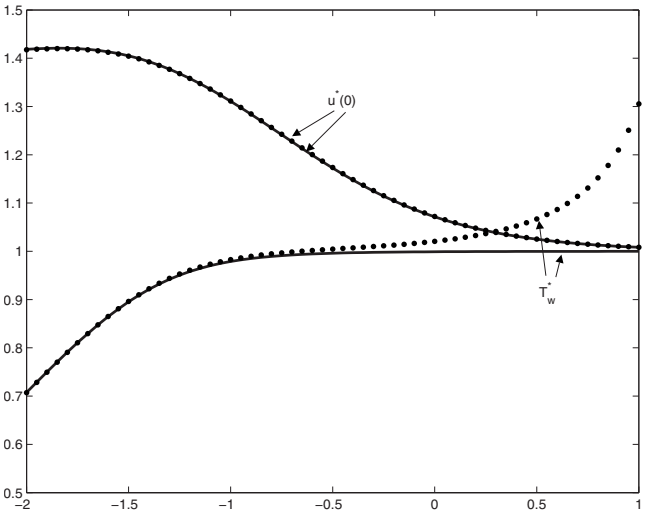

FIG. 14. Average velocity and temperature $(u(0)/u_r,\ T_w/T_r)$ vs the Knudsen number in logarithmic scale in the force-driven compressible Poiseuille gas flow ($\varepsilon_{h_w}=0.3$). The (●) symbols represent the NCCR theory, while the (–) represents the compressible Navier–Stokes–Fourier result.

ACKNOWLEDGMENTS

This work was supported by the Priority Research Centers Program through the National Research Foundation of Korea (NRF) funded by the Ministry of Education, Science and Technology (Grant No. 2009-0094016) and partially by the Degree and Research Center for Aerospace Green Technology (DRC) of the Korea Aerospace Research Institute (KARI), funded by the Korea Research Council of Fundamental Science and Technology (KRCF).

APPENDIX A: QUALITATIVE EQUIVALENCE OF LANGMUIR AND MAXWELL SLIP (JUMP) MODELS

An alternative way of including slip is to make a correction based on the degree of nonequilibrium near the wall surface. This idea originates from the work of Maxwell[32] and subsequent work by Smoluchowski.[33] After the degree of

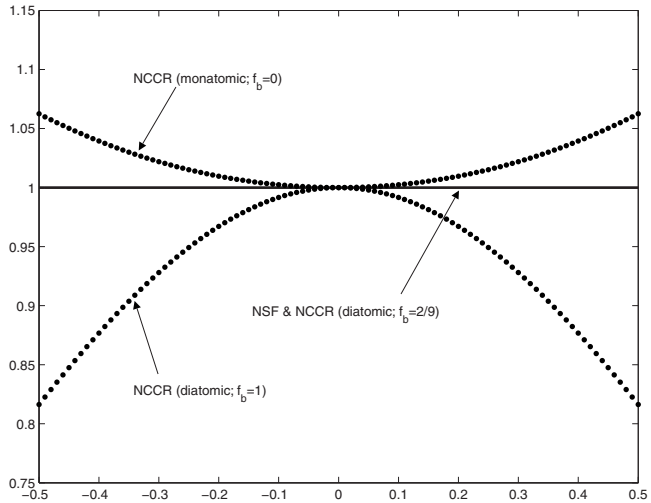

FIG. 16. Effect of the bulk viscosity on the pressure distribution in diatomic gases ($f_b=0.0, 2/9, 1.0$; $\varepsilon_h=0.6$). The horizontal axis represents the distance s^*, while the vertical axis represents the pressure $p(s^*)/p(0)$.

nonequilibrium (e.g., shear stress) near the wall surface is taken as linear, the following velocity slip and temperature jump boundary conditions are proposed:

$$u(y=h/2)=\sigma_V l\cdot(-)\left.\frac{du}{dy}\right]_{y=h/2} \tag{A1}$$

$$\text{and}\quad T(y=h/2)=T_w+\sigma_T l\cdot(-)\left.\frac{dT}{dy}\right]_{y=h/2}.$$

With the definition of the mean free path $l=\sqrt{\pi/2}\,\eta/(\rho\sqrt{RT})$, the conditions are reduced to, in the present problem,

$$u^*(y^*=1/2)=\sigma_V\ \mathrm{Kn}\cdot(-)\left.\frac{du^*}{dy^*}\right]_{y^*=1/2} \tag{A2}$$

$$\text{and}\quad T^*(y^*=1/2)=T_w^*+\sigma_T\ \mathrm{Kn}\cdot(-)\left.\frac{dT^*}{dy^*}\right]_{y^*=1/2}.$$

When the velocity profile in Navier–Stokes–Fourier theory (3.3) or Eq. (3.21) is combined with the Maxwell slip model in Eq. (A2), it can be written as

$$u^*(y^*=1/2)=\sigma_V\ \mathrm{Kn}\cdot(-)\left.\frac{du^*}{dy^*}\right]_{y^*=1/2}$$

$$=\sigma_V\ \mathrm{Kn}\frac{\varepsilon_h}{2N_\delta}T_w^*=u^*(0)-T_w^*\frac{\varepsilon_h}{8N_\delta}. \tag{A3}$$

Then, it is straightforward to show that with an equivalence relation

$$\alpha_{M_V}=\frac{1}{1+4\sigma_V\ \mathrm{Kn}}, \tag{A4}$$

the following velocity profile is exactly the same as the Langmuir slip model (3.5) or Eq. (3.23):

$$u^*(y^*)=u^*(0)(1-4\alpha_{M_V}y^{*2})\quad\text{and}\quad\frac{T_w^*}{8}\frac{\varepsilon_h}{N_\delta}=\alpha_{M_V}u^*(0). \tag{A5}$$

Similarly, when the temperature profile in Navier–Stokes–Fourier theory (3.8) or Eq. (3.26) is combined with the Maxwell jump model in Eq. (A2), it can be written as

$$T^*(y^*=1/2)=T_w^*+\sigma_T\ \mathrm{Kn}\frac{(\gamma-1)\mathrm{Pr}\ T_w^{*3}M^2\varepsilon_h^2}{12N_\delta^2}$$

$$=T^*(0)-\frac{(\gamma-1)\mathrm{Pr}\ T_w^{*3}M^2\varepsilon_h^2}{192N_\delta^2}. \tag{A6}$$

Then, it is straightforward to show that with an equivalence relation

$$\alpha_{M_T}=\frac{1}{1+8\sigma_T\ \mathrm{Kn}}, \tag{A7}$$

the following temperature profile is exactly the same as the Langmuir jump model (3.10) or Eq. (3.28):

$$T^*(y^*)=T^*(0)-16\alpha_{M_T}[T^*(0)-T_w^*]y^{*4} \tag{A8}$$

$$\text{and}\quad\frac{\pi(\gamma-1)\mathrm{Pr}\ \varepsilon_h^2T_w^{*3}}{384\gamma\ \mathrm{Kn}^2}=\alpha_{M_T}[T^*(0)-T_w^*].$$

This completes the proof of the qualitative equivalence of the Langmuir and Maxwell slip (jump) models.

APPENDIX B: MATHEMATICAL ANALYSIS ON THE EXISTENCE OF THE TEMPERATURE MINIMUM AT THE CENTERLINE

The governing equation (4.1) with the essential components may be expressed in another instructive form, with the assumptions of the relaxation time approximation and Maxwell molecule,

$$\frac{d}{ds^*}\begin{bmatrix}u^*\\p^*\\T^*\\\Pi_{xy}^*\\Q_y^*\end{bmatrix}=p^*\begin{bmatrix}-[\Pi_{xy}^*]_0T_w^*\\0\\-(\Delta T/T_r)[Q_y^*]_0T_w^*\\\varepsilon_h/N_\delta\\\mathrm{Pr}\ \mathrm{Ec}[\Pi_{xy}^*]_0^2T_w^*\end{bmatrix}+\varepsilon_hN_\delta[\Pi_{xy}^*]_0\begin{bmatrix}0\\(4/3)p^*\\[(\gamma-1)/\gamma]T^*\\0\\0\end{bmatrix}. \tag{B1}$$

The corresponding equations in the classical compressible Navier–Stokes–Fourier case are simplified into

$$\frac{d}{ds^*}\begin{bmatrix}u^*\\p^*\\T^*\\\Pi_{xy}^*\\Q_y^*\end{bmatrix}=\begin{bmatrix}-\Pi_{xy}^*T_w^*\\0\\-(\Delta T/T_r)Q_y^*T_w^*\\\varepsilon_h/N_\delta\\\mathrm{Pr}\ \mathrm{Ec}\ \Pi_{xy}^{*2}T_w^*\end{bmatrix}. \tag{B2}$$

In this case, it is straightforward to show that

$$\left.\frac{dT^*}{ds^*}\right]_{s^*=0}=\left.\frac{d^2T^*}{ds^{*2}}\right]_{s^*=0}=\left.\frac{d^3T^*}{ds^{*3}}\right]_{s^*=0}=0 \tag{B3}$$

$$\text{and}\quad\left.\frac{d^4T^*}{ds^{*4}}\right]_{s^*=0}=-\frac{(\gamma-1)}{\gamma}\pi\ \mathrm{Pr}\ T_w^{*3}\frac{\varepsilon_h^2}{\mathrm{Kn}^2},$$

implying the existence of the temperature maximum near the centerline. On the other hand, when the full set of Eq. (B1) is considered, that is, in the case of nonclassical NCCR theory, it can be proved that

$$\left.\frac{dT^*}{ds^*}\right]_{s^*=0}=0\quad\text{and}\quad\left.\frac{d^2T^*}{ds^{*2}}\right]_{s^*=0}=\frac{(\gamma-1)}{\gamma}T^*(0)\varepsilon_h^2. \tag{B4}$$

The temperature near the centerline is now at a minimum and the concavity is affected mainly by the value of ε_h^2. This completes the proof of the existence of the central temperature minimum in the force-driven Poiseuille gas flow.

APPENDIX C: PHENOMENOLOGICAL INTERPRETATION ON THE NATURE OF THE CONTINUOUS SYMMETRIC CONDITION AT THE CENTERLINE

The properties of conserved variables near the centerline $y=0$ must satisfy the continuous symmetric condition arising from the flow geometry in the present problem. In order that the conserved variables $u(y), T(y), p(y)$ may be continuous, symmetric, and differentiable at $y=0$, their first derivatives at $y=0$ must vanish. This condition is equivalent to a physical requirement that all components of the thermodynamic driving forces defined for species i,

$$[\nabla \mathbf{u}]^{(2)}, \quad \nabla \cdot \mathbf{u}, \quad \nabla T, \quad (\nabla \hat{\mu}_i)_T + \mathbf{a} - \mathbf{a}_i - \nabla p/\rho \tag{C1}$$

vanish in the present problem as well, since spatial gradients of all the conserved variables near the centerline are zero and force field **a** exerted on single component of gas is *uniform* (in space). In Eq. (C1), $\hat{\mu}_i$ represents the material part of the chemical potential of species i (Ref. 2, p. 520; Ref. 36, p. 108; Ref. 37), which is defined as the change in Gibbs free energy with respect to change in the amount of component. It, in turn, means that

$$\mathbf{\Pi}(0)=0, \quad \mathbf{Q}(0)=0, \tag{C2}$$

which is the direct consequence of a fundamental physical observation that the stress and heat flux are produced by thermodynamic driving forces.

This interpretation of the continuous symmetric condition at the centerline can also be explained by considering the kinetic Boltzmann equation. Under acceleration of gas molecules driven by uniform force in open space free from the gas-surface molecular interaction, the following Maxwell–Boltzmann distribution:

$$f^M(t,v_x,v_y,v_z) = n\left(\frac{m}{2\pi k_B T}\right)^{3/2} e^{-(m/2k_BT)[(v_x-at)^2+v_y^2+v_z^2]} \tag{C3}$$

satisfies the kinetic Boltzmann equation exactly

$$\frac{\partial f}{\partial t} + v_y \frac{\partial f}{\partial y} + a\frac{\partial f}{\partial v_x} = C[f] \tag{C4}$$

since

$$\frac{\partial f^M}{\partial y} = 0 \quad \text{(homogeneity)}, \quad C[f^M]=0 \quad \text{(definition)},$$
$$\frac{\partial f^M}{\partial t} + a\frac{\partial f^M}{\partial v_x} = 0 \quad \text{(algebra)}. \tag{C5}$$

When the gas-surface molecular interaction at the wall is taken into account, the Maxwell–Boltzmann distribution (C3) is changed into

$$f^M(v_x,v_y,v_z) = n(y=0)\left[\frac{m}{2\pi k_B T(y=0)}\right]^{3/2} \times e^{-[m/2k_BT(y=0)]\{[v_x-u(y=0)]^2+v_y^2+v_z^2\}} \tag{C6}$$

at the centerline $y=0$, which satisfies the following stationary kinetic Boltzmann equation exactly:

$$v_y \frac{\partial f}{\partial y} = C[f]. \tag{C7}$$

Notice that the only role of uniform force a in this situation is to assign nonzero uniform streamwise velocity $u(y=0)$. However, when local nonequilibrium distributions away from the centerline $y=0$ associated with nonzero slope du/dy are considered, the force term $a\partial f/\partial v_x$ must be retained in the kinetic equation. For the Maxwell–Boltzmann distribution at the centerline (C6), it is straightforward to show

$$\Pi_{xy}(0) \equiv \langle m[\mathbf{cc}]_{xy}^{(2)} f^M \rangle = m\langle c_x c_y f^M \rangle = 0,$$
$$Q_y(0) \equiv \left\langle \tfrac{1}{2} m c^2 c_y f^M \right\rangle = 0, \tag{C8}$$

$$\Pi_{yy}(0) \equiv \langle m[\mathbf{cc}]_{yy}^{(2)} f^M \rangle = m\left\langle \left(c_y^2 - \tfrac{1}{3}c^2\right) f^M \right\rangle = 0,$$
$$Q_x(0) \equiv \left\langle \tfrac{1}{2} m c^2 c_x f^M \right\rangle = 0. \tag{C9}$$

APPENDIX D: ROLE OF BULK VISCOSITY IN DIATOMIC GASES

In the case of diatomic gases, the following Boltzmann–Curtiss kinetic equation with a moment of inertia I and an angular momentum **j** may be considered:

$$\left[\frac{\partial}{\partial t} + \mathbf{v}\cdot\nabla + \mathbf{a}\cdot\nabla_{\mathbf{v}} + \frac{j}{I}\frac{\partial}{\partial \psi}\right] f(\mathbf{v},\mathbf{r},\mathbf{j},\psi,t) = C[f]. \tag{D1}$$

In this equation, ψ, j, and $C[f]$ represent the azimuth angle associated with the orientation of the molecule, the magnitude of the angular momentum vector **j**, and the collision integral, respectively. Then, the following algebraic constitutive relations can be derived:[4,6,7]

$$\begin{bmatrix}0\\0\\0\end{bmatrix}=-\begin{bmatrix}\underline{2(p+\Delta)[\nabla\mathbf{u}]^{(2)}}+2[\mathbf{\Pi}\cdot\nabla\mathbf{u}]^{(2)}\\ \underline{p\,\nabla\cdot\mathbf{u}}+3(\Delta\mathbf{I}+\mathbf{\Pi}):\nabla\mathbf{u}\\ \underline{(p+\Delta)C_p\nabla T}+\mathbf{\Pi}\cdot C_p\nabla T+\mathbf{Q}\cdot\nabla\mathbf{u}-a\mathbf{I}\cdot\mathbf{\Pi}\end{bmatrix}+\begin{bmatrix}\mathbf{\Lambda}^{(\Pi)}\\ \mathbf{\Lambda}^{(\Delta)}\\ \mathbf{\Lambda}^{(Q)}\end{bmatrix}. \tag{D2}$$

In these expressions, the variable $\Delta\equiv\mathrm{Tr}(\mathbf{P})/3-p$ denotes the excess normal stress; the corresponding Newtonian law is $\Delta_0=-\eta_b\nabla\cdot\mathbf{u}$, where η_b denotes the bulk viscosity. The constant f_b represents the ratio of the bulk viscosity to the shear viscosity. For the force-driven Poiseuille flow within the rectangular channel (infinitely long width and length), the conservation laws and the constitutive equation of stress are reduced to

$$\frac{d}{dy}\begin{bmatrix}\Pi_{xy}\\ p+\Pi_{yy}+\Delta\\ \Pi_{yz}\\ \Pi_{xy}u+Q_y\end{bmatrix}=\begin{bmatrix}\rho a\\ 0\\ 0\\ \rho a u\end{bmatrix}, \tag{D3}$$

$$\begin{bmatrix}0\\0\\0\\0\\0\\0\end{bmatrix}=\frac{1}{\eta}\begin{bmatrix}(4/3)[\Pi_{xy}]_0[\Pi_{xy_0}]_0\\ -(2/3)[\Pi_{xy}]_0[\Pi_{xy_0}]_0\\ -(2/3)[\Pi_{xy}]_0[\Pi_{xy_0}]_0\\ (p+[\Pi_{yy}]_0+[\Delta]_0)[\Pi_{xy_0}]_0\\ [\Pi_{yz}]_0[\Pi_{xy_0}]_0\\ 0\\ 3[\Pi_{xy}]_0[\Pi_{xy_0}]_0\end{bmatrix}-\frac{p}{\eta}\begin{bmatrix}[\Pi_{xx}]_0\\ [\Pi_{yy}]_0\\ [\Pi_{zz}]_0\\ [\Pi_{xy}]_0\\ [\Pi_{xz}]_0\\ [\Pi_{yz}]_0\\ \eta[\Delta]_0/\eta_b\end{bmatrix}F(p,T,\mathbf{\Pi},\Delta,\mathbf{Q},\ldots).$$

When the same method developed for monatomic gases is used, it can be shown that the y-momentum equation in the conservation law of the one-dimensional force-driven Poiseuille flow is reduced to

$$\frac{d}{dy}(p+\Pi_{yy}+\Delta)=0 \quad \text{or} \quad p+[\Pi_{yy}]_0+[\Delta]_0=p_m. \tag{D4}$$

Also, from three essential algebraic constitutive relations,

$$\begin{bmatrix}0\\0\\0\end{bmatrix}=\begin{bmatrix}-(2/3)[\Pi_{xy}]_0[\Pi_{xy_0}]_0\\ (p+[\Pi_{yy}]_0+[\Delta]_0)[\Pi_{xy_0}]_0\\ 3f_b[\Pi_{xy}]_0[\Pi_{xy_0}]_0\end{bmatrix}-p\begin{bmatrix}[\Pi_{yy}]_0\\ [\Pi_{xy}]_0\\ [\Delta]_0\end{bmatrix}F(p,T,\mathbf{\Pi},\Delta,\mathbf{Q},\ldots), \tag{D5}$$

the following kinematic constraint on the viscous stresses in the velocity shear flow can be written as (refer to Refs. 6 and 7 for details):

$$[\Pi_{xy}]_0^2=-\tfrac{3}{2}\left[\left(1-\tfrac{9}{2}f_b^2\right)[\Pi_{yy}]_0+p\right][\Pi_{yy}]_0 \quad \text{and} \quad [\Delta]_0=-\tfrac{9}{2}f_b[\Pi_{yy}]_0. \tag{D6}$$

When Eq. (D4) is combined with the second equation of Eq. (D6), it is reduced to

$$p+\left(1-\tfrac{9}{2}f_b\right)[\Pi_{yy}]_0=p_m. \tag{D7}$$

This simple relation indicates that the pressure remains constant when $f_b=2/9$. Furthermore, the pressure at the centerline p_m is at a maximum $p_{\max}$ when $f_b>2/9$ since the property $[\Pi_{yy}]_0$ is negative, resulting in the convex pressure distribution near the centerline. On the other hand, the pressure at the centerline p_m is at a minimum $p_{\min}$ when $f_b<2/9$, resulting in the concave pressure distribution. In fact, when Eq. (D7) is combined with the stress constraint (D6), it is straightforward to show $(0\le y\le h/2)$,

$$\frac{[\Pi_{xy}]_0}{p_{\min}}=\mathrm{sign}(\Pi_{xy_0})\left\{\frac{3}{(2-9f_b)}\left[\frac{(2-9f_b^2)}{(2-9f_b)}\left(1-\frac{p}{p_{\min}}\right)+\frac{p}{p_{\min}}\right]\left(\frac{p}{p_{\min}}-1\right)\right\}^{1/2} \quad \text{when} \quad 0\le f_b<\frac{2}{9}, \tag{D8}$$

$$\frac{[\Pi_{xy}]_0}{p_{\max}}=\mathrm{sign}(\Pi_{xy_0})\left\{\frac{3}{(9f_b-2)}\left[\frac{(9f_b^2-2)}{(9f_b-2)}\left(1-\frac{p}{p_{\max}}\right)+\frac{p}{p_{\max}}\right]\left(1-\frac{p}{p_{\max}}\right)\right\}^{1/2} \quad \text{when} \quad f_b>\frac{2}{9}. \tag{D9}$$

When the bulk viscosity ratio f_b is equal to 1, the type of the stress constraint turns into a hyperbola. Then, Eq. (D9) is reduced to a compact form

$$\frac{[\Pi_{xy}]_0}{p_{\max}} = \mathrm{sign}(\Pi_{xy_0})\sqrt{\frac{3}{7}\left(1-\frac{p}{p_{\max}}\right)}. \tag{D10}$$

The x-momentum equation, $d\Pi^*_{xy}/ds^* = \varepsilon_h p^*/N_\delta$, combined with Eq. (D10), is reduced to an ordinary differential equation, in dimensionless form,

$$\frac{1}{p^*}d\left[\mathrm{sign}(\Pi_{xy_0})\sqrt{\frac{3}{7}(1-p^*)}\right] = \varepsilon_h ds^*. \tag{D11}$$

By using an integral formula,

$$\int \frac{1}{p^*}d(\sqrt{1-p^*}) = \tanh^{-1}\sqrt{1-p^*}, \tag{D12}$$

the differential equation yields the following analytical solution for the pressure and the stresses in diatomic gas with $f_b=1$ $(S^* \equiv \sqrt{2/3}\varepsilon_h s^*)$:

$$p^*(S^*) = 1-\tanh^2\left(\sqrt{\frac{7}{2}}S^*\right),$$

$$[\Pi^*_{yy}(S^*)]_0 = -\frac{2}{7N_\delta}\tanh^2\left(\sqrt{\frac{7}{2}}S^*\right), \tag{D13}$$

$$[\Delta^*(S^*)]_0 = \frac{9}{7N_\delta}\tanh^2\left(\sqrt{\frac{7}{2}}S^*\right),$$

$$[\Pi^*_{xy}(S^*)]_0 = \frac{1}{N_\delta}\sqrt{\frac{3}{7}}\tanh\left(\sqrt{\frac{7}{2}}S^*\right).$$

Note that the distribution of the sum of pressure and excess normal stress remains concave, while the pressure distribution remains convex,

$$p^*(S^*) + N_\delta[\Delta^*(S^*)]_0 = 1+\tfrac{2}{7}\tanh^2\left(\sqrt{\tfrac{7}{2}}S^*\right). \tag{D14}$$

[1] C. Truesdell and W. Noll, *The Non-Linear Field Theories of Mechanics* (Springer, Heidelberg, 2003).
[2] B. C. Eu, *Kinetic Theory and Irreversible Thermodynamics* (Wiley, New York, 1992).
[3] B. C. Eu, *Nonequilibrium Statistical Mechanics: Ensemble Method* (Kluwer Academic, Dordrecht, 1998).
[4] B. C. Eu, *Generalized Thermodynamics: The Thermodynamics of Irreversible Processes and Generalized Hydrodynamics* (Kluwer Academic, Dordrecht, 2002).
[5] R. S. Myong, "Thermodynamically consistent hydrodynamic computational models for high-Knudsen-number gas flows," Phys. Fluids **11**, 2788 (1999).
[6] R. S. Myong, "A generalized hydrodynamic computational model for rarefied and microscale diatomic gas flows," J. Comput. Phys. **195**, 655 (2004).
[7] R. S. Myong, "Coupled nonlinear constitutive models for rarefied and microscale gas flows: Subtle interplay of kinematics and dissipation effects," Continuum Mech. Thermodyn. **21**, 389 (2009).
[8] G. Karniadakis, A. Beskok, and N. Aluru, *Microflows and Nanoflows: Fundamentals and Simulation* (Springer, New York, 2005).
[9] J. M. Reese, M. A. Gallis, and D. A. Lockerby, "New directions in fluid dynamics: Non-equilibrium aerodynamic and microsystem flows," Philos. Trans. R. Soc. London, Ser. A **361**, 2967 (2003).
[10] D. A. Lockerby, J. M. Reese, and M. A. Gallis, "The usefulness of higher-order constitutive relations for describing the Knudsen layer," Phys. Fluids **17**, 100606 (2005).
[11] L. O'Hare, D. A. Lockerby, J. M. Reese, and D. R. Emerson, "Near-wall effects in rarefied gas micro-flows: Some modern hydrodynamic approaches," Int. J. Heat Fluid Flow **28**, 37 (2007).
[12] K. Xu, "Super-Burnett solutions for Poiseuille flow," Phys. Fluids **15**, 2077 (2003).
[13] K. Xu, H. Liu, and J. Jiang, "Multiple temperature kinetic model for continuum and near continuum flows," Phys. Fluids **19**, 016101 (2007).
[14] Z. L. Guo and K. Xu, "Numerical validation of Brenner's hydrodynamic model by force driven Poiseuille flow," Adv. Appl. Math. and Mech. **1**, 391 (2009).
[15] M. Torrilhon, "Two-dimensional bulk microflow simulations based on regularized Grad's 13-moment equations," Multiscale Model. Simul. **5**, 695 (2006).
[16] M. Torrilhon and H. Struchtrup, "Boundary conditions for regularized 13-moment-equations for micro-channel flows," J. Comput. Phys. **227**, 1982 (2008).
[17] P. Taheri, M. Torrilhon, and H. Struchtrup, "Couette and Poiseuille microflows: Analytical solutions for regularized 13-moment equations," Phys. Fluids **21**, 017102 (2009).
[18] M. Tij and A. Santos, "Perturbation analysis of a stationary nonequilibrium flow generated by an external force," J. Stat. Phys. **76**, 1399 (1994).
[19] M. Malek Mansour, F. Baras, and A. L. Garcia, "On the validity of hydrodynamics in plane Poiseuille flows," Physica A **240**, 255 (1997).
[20] F. J. Uribe and A. L. Garcia, "Burnett description of plane Poiseuille flow," Phys. Rev. E **60**, 4063 (1999).
[21] Y. Zheng, A. L. Garcia, and B. J. Alder, "Comparison of kinetic theory and hydrodynamics for Poiseuille flow," J. Stat. Phys. **109**, 495 (2002).
[22] S. Ansumali, "Minimal kinetic modeling of hydrodynamics," Doctor of Technical Sciences dissertation, Swiss Federal Institute of Technology, Zurich, 2004.
[23] H. Grad, "On the kinetic theory of rarefied gases," Commun. Pure Appl. Math. **2**, 331 (1949).
[24] C. D. Levermore, "Moment closure hierarchies for kinetic theories," J. Stat. Phys. **83**, 1021 (1996).
[25] M. Al-Ghoul and B. C. Eu, "Generalized hydrodynamic theory of shock waves: Mach-number dependence of inverse shock width for nitrogen gas," Phys. Rev. Lett. **86**, 4294 (2001).
[26] M. Al-Ghoul and B. C. Eu, "Nonequilibrium partition function in the presence of heat flow," J. Chem. Phys. **115**, 8481 (2001).
[27] B. C. Eu, R. E. Khayat, G. D. Billing, and C. Nyeland, "Nonlinear transport coefficients and plane Couette flow of a viscous, heat-conducting gas between two plates at different temperatures," Can. J. Phys. **65**, 1090 (1987).
[28] R. S. Myong, "Gaseous slip model based on the Langmuir adsorption isotherm," Phys. Fluids **16**, 104 (2004).
[29] R. S. Myong, D. A. Lockerby, and J. M. Reese, "The effect of gaseous slip on microscale heat transfer: An extended Graetz problem," Int. J. Heat Mass Transfer **49**, 2502 (2006).
[30] H. M. Kim, D. Kim, W. T. Kim, P. S. Chung, and M. S. Jhon, "Langmuir slip model for air bearing simulation using the lattice Boltzmann method," IEEE Trans. Magn. **43**, 2244 (2007).
[31] S. Chen and Z. Tian, "Simulation of thermal micro-flow using lattice Boltzmann method with Langmuir slip model," Int. J. Heat Fluid Flow **31**, 227 (2010).

[32]J. C. Maxwell, "On stresses in rarefied gases arising from inequalities of temperature," Philos. Trans. R. Soc. London **170**, 231 (1879).
[33]M. von Smoluchowski, "Uber den temperauresprung bei warmeleitung in gasen," Akad. Wiss. Wien **107**, 304 (1898).
[34]P. L. Bhatnagar, E. P. Gross, and M. Krook, "A model for collision processes in gases, I," Phys. Rev. **94**, 511 (1954).
[35]T. J. Bright and Z. M. Zhang, "Common misperceptions of the hyperbolic heat equation," J. Thermophys. Heat Transfer **23**, 601 (2009).
[36]K. A. Dill and S. Bromberg, *Molecular Driving Forces: Statistical Thermodynamics in Chemistry & Biology* (Garland Science, New York, 2002).
[37]B. C. Eu and M. Al-Ghoul, *Chemical Thermodynamics with Examples for Nonequilibrium Processes* (World Scientific, Singapore, 2010).